



Research paper

Design, synthesis, and biological evaluation of hederagenin derivatives with improved aqueous solubility and tumor resistance reversal activity



Binghua Wang¹, Shuqi Liu¹, Wentao Huang, Mengxin Ma, Xiaoqian Chen, Wenxuan Zeng, Kaicheng Liang, Hongbo Wang*, Yi Bi**, Xiaopeng Li

School of Pharmacy, Key Laboratory of Molecular Pharmacology and Drug Evaluation (Yantai University), Ministry of Education, Collaborative Innovation Center of Advanced Drug Delivery System and Biotech Drugs in Universities of Shandong, Yantai University, Yantai, 264005, PR China

ARTICLE INFO

Article history:

Received 22 September 2020

Received in revised form

5 December 2020

Accepted 14 December 2020

Available online 17 December 2020

Keywords:

Hederagenin

PEGylated derivatives

Synthesis

Tumor resistance reversal activity

Aqueous solubility

P-glycoprotein

ABSTRACT

Multidrug resistance (MDR) has become a major obstacle to malignancies treatment by chemotherapeutic drugs, therefore, it is important to develop MDR reversal agents with high activity. We have previously found that the hederagenin (HD) derivative **HBQ** showed good tumor MDR reversal activity *in vitro* and *in vivo* but had poor solubility. In this study, to enhance the aqueous solubility and tumor MDR reversal activity of **HBQ**, three series of HD derivatives were designed and synthesized. Nitrogen-containing heterocyclic-substituted, PEGylated, and ring-A substituted derivatives significantly reversed the MDR phenotype of KBV (multidrug-resistant oral epidermoid carcinoma) cells toward paclitaxel at a concentration of 10 μ M in MTT assays. The PEGylated derivatives **10c–10e** had increased aqueous solubility compared with **HBQ** by 18–657 fold, while maintaining tumor MDR reversal activity. The most *in vitro* active compound **10c** possessed good chemical stability to an esterase over 24 h and enhanced the sensitivity of KBV cells to paclitaxel and vincristine with IC₅₀ values of 4.58 and 0.79 nM, respectively. Mechanism studies indicated that compound **10c** increased the accumulation of P-glycoprotein (P-gp) substrates rhodamine 123 and Flutax1 in KBV cells and MCF-7T (paclitaxel-resistant breast carcinoma) cells, that is to say, compound **10c** exerted the reversal effect of tumor MDR by inhibiting the efflux function of P-gp. Finally, the structure–activity relationships were further investigated by analyzing the relationship between structure and tumor MDR reversal activity of HD derivatives. This study highlights the potential of PEGylated HD derivatives such as compound **10c** for the development of tumor MDR reversal agents and provides information for the further improvement of the aqueous solubility and tumor MDR reversal activity of HD derivatives in the future.

© 2020 Elsevier Masson SAS. All rights reserved.

1. Introduction

Tumor multidrug resistance (MDR) phenotype refers to the cross-resistance of tumor cells to antitumor drugs with different structures and mechanisms of action, which is the main reason for the failure of tumor chemotherapy [1,2]. The majority of antitumor drugs have a small difference between the dose to achieve a therapeutic effect and the dose that produce toxicity. Therefore, it is

particularly important to overcome the MDR phenotype, and the development of MDR reversal agents has become the focus of current tumor treatment [3–5]. The overexpression of P-glycoprotein (P-gp) is considered to be one of the major mechanisms that induce MDR. P-gp is a member of the family of ATP binding cassette (ABC) transporters [6,7], and it uses ATP hydrolysis to drive the efflux of antitumor drugs, thus decreasing the efficacy of chemotherapy and leading to MDR [8,9]. Therefore, inhibition of P-gp is a potential method to overcome MDR, but it has only achieved limited success in clinical research [10]. As a first-generation P-gp inhibitor, verapamil (Fig. 1) significantly enhances the sensitivity of drug-resistant tumor cells to chemotherapeutic drugs, such as paclitaxel, but has considerable cardiac toxicity. Second and third-generation inhibitors such as dofequidar (MS-209, Fig. 1),

* Corresponding author.

** Corresponding author.

E-mail addresses: hongbowangyt@gmail.com (H. Wang), beeyee_413@163.com (Y. Bi).

¹ These authors have equally contributed to the work.

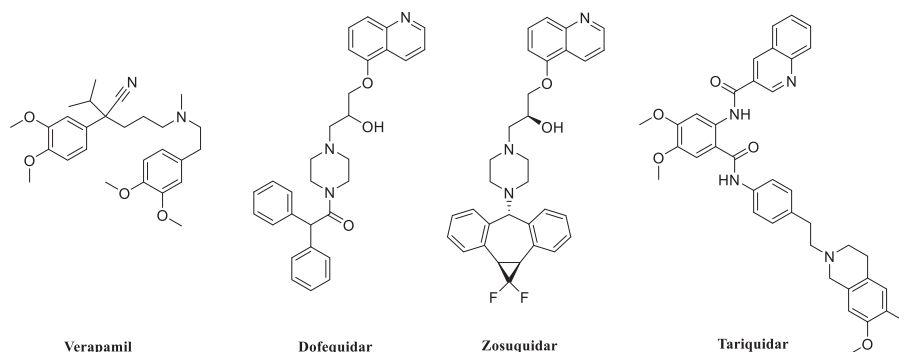


Fig. 1. Chemical structures of verapamil, dofequidar, zosuquidar and tariquidar.

zosuquidar (LY335979, Fig. 1) and tariquidar (XR9576, Fig. 1), are limited in clinical application because of inherent toxicity or poor potency [11,12]. Therefore, the search for novel tumor MDR reversal agents with strong activity and low toxicity has become important in the field of malignant tumor treatment.

Compared with the previous three generations of P-gp inhibitors, natural products have high chemical diversity and low toxicity, which are considered to be a reliable source of potential P-gp inhibitors and termed “the fourth-generation inhibitors” [13,14]. Many different structural types of natural products have been shown to have tumor MDR reversal activity with less toxicity, including flavonoids [13,15], alkaloids [14,15], terpenes [15,16], and coumarins [15]. Most notably, several triterpenoids with various structures could effectively inhibit the function of P-gp in different drug-resistant cells [17]. Nabekura et al. reported that glycyrrhetic acid (Fig. 2) inhibited the function of P-gp in KB-C2 (multidrug-resistant human epidermal carcinoma) cells, and MDR associated protein 1 (MRP1) in KB/MRP (human MRP1 gene-transfected multidrug-resistant epidermal carcinoma) cells, which enhanced the sensitivity of KB-C2 cells to vincristine and KB/MRP cells to doxorubicin [18]. Ren et al. reported that the 24R-ocotillol-type amide derivative OR1 (Fig. 2) significantly enhanced the sensitivity of drug-resistant tumor cells to paclitaxel *in vitro* and *in vivo* and inhibited the efflux of the P-gp substrate rhodamine 123 in KBV (multidrug-resistant oral epidermoid carcinoma) cells by increasing P-gp ATPase activity [17]. However, most of the natural products with good activity had poor aqueous solubility and low bioavailability, which has limited their applications [19]. Increasing the aqueous solubility of natural products is one of the important ways to improve the druggability of compounds.

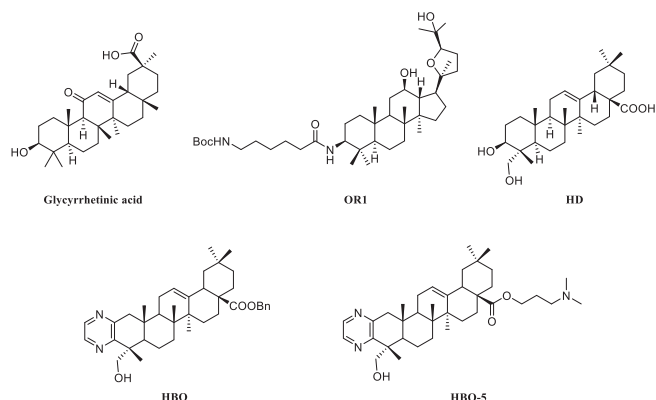


Fig. 2. Chemical structures of glycyrrhetic acid, OR1, HD, HBQ and HBQ-5.

Hederagenin (HD, Fig. 2), first found in the leaves of English ivy in 1849, is an oleanane-type pentacyclic triterpene, which has been found to have a variety of pharmacological effects, including anti-tumor [20], anti-inflammatory [21], antidepressant [22], and anti-neurodegenerative [23] effects. In particular, many researchers have modified the structure of HD, and some of the derivatives could enhance the antitumor activity of HD [24–27]. Our group first discovered that HD derivatives have tumor MDR reversal activity. The derivative HBQ (Fig. 2), obtained by structural modification of HD, had good tumor MDR reversal activity both *in vitro* and *in vivo* [28]. HBQ had no obvious cytotoxicity *in vitro* when used alone at a concentration of 10 μ M, and significantly increased the anti-proliferative activity of paclitaxel in drug-resistant KBV cells with an IC_{50} value of 2.39 ± 0.74 nM when combined with 100 nM paclitaxel. In addition, the tumor growth inhibition rate was 41.88% when HBQ (10 mg/kg) was combined with paclitaxel (30 mg/kg) in a drug-resistant KBV cell xenograft nude mice model. HBQ can reverse MDR by stimulating the ATPase activity of P-gp and then competing with the chemotherapeutic drugs to bind to P-gp. However, the poor solubility of HBQ has limited its further use. To improve the aqueous solubility of HBQ, we synthesized a series of HBQ derivatives, of which HBQ-5 (Fig. 2), is a representative derivative. However, HBQ-5 had poor activity *in vivo* compared with HBQ and limited solubility [29]. Therefore, further structural modification to improve the druggability of HBQ, while maintaining or enhancing the activity, was investigated.

To overcome the poor aqueous solubility of small-molecule drugs, polyethylene glycol (PEG, Fig. 3) has received extensive attention in the structural modification of small-molecule drugs in recent years [30,31]. PEG comprises a repeating ethylene glycol subunit structure and has good biocompatibility and high aqueous solubility. PEGylation has been shown to improve the aqueous solubility and pharmacokinetic properties of antitumor drugs such as adriamycin, paclitaxel, and camptothecin [30,32,33]. NKTR-102 (Fig. 3), obtained by linking irinotecan to a four-arm PEG molecule, has an extended half-life and increased area under the concentration time-curve (AUC) compared with irinotecan, and is in phase III clinical trials for metastatic breast cancer [34]. Medina-O'Donnell et al. have designed and synthesized a series of PEGylated derivatives of maslinic acid (MA). The aqueous solubility of the derivatives was higher than that of MA, and increased with length of PEG chains, the compound MA-8 (Fig. 3) had 477-fold higher solubility than MA [35]. Thus, PEGylation may be an effective method to improve the aqueous solubility of HBQ derivatives.

Therefore, in this study, to enhance the aqueous solubility and tumor MDR reversal activity of HBQ, and to further explore the structure–activity relationships (SARs), we designed and synthesized several series of HD derivatives. The designed strategies are

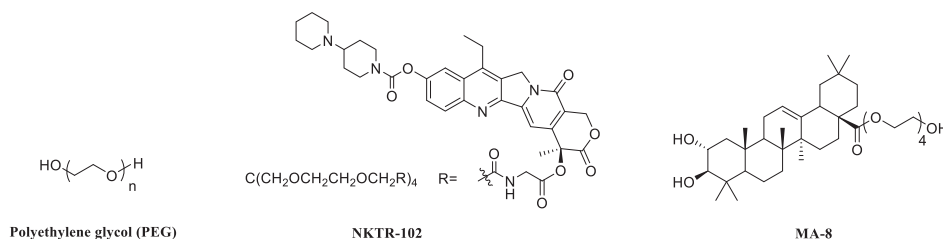


Fig. 3. Chemical structures of PEG, NKTR-102, and MA-8.

shown in Fig. 4. First, several PEG molecules with different chain lengths were introduced at the C-23 and C-28 positions of **HBQ** to explore the influence of different chain lengths of PEG and different modification positions on the solubility and activity of the target compounds. In addition, the presence of nitrogen-containing heterocycles such as piperazinyl, substituted piperazinyl, and morpholinyl groups has been shown to enhance the tumor MDR reversal activity of compounds [12,36], and previous SAR studies in our group have indicated that the activity was improved when C-28 was substituted with a nitrogen-containing group. Therefore, we designed and synthesized derivatives with nitrogen-containing heterocycles substituted at C-28 in an attempt to improve the activity of **HBQ**. Moreover, based on the good activity of **HBQ**, in which ring-A is a fused pyrazine, the ring-A fused pyrazole derivatives were designed by using the principles of bioisosterism [37,38]. In addition, to further enrich the SARs, ring-A fused methyl thiazole analogues were designed. Herein, we report the synthesis of these derivatives and the evaluation of their tumor MDR reversal activities *in vitro*. In addition, the aqueous solubility, *in vitro* stability, and mechanism of action of compound **10c** were also investigated.

2. Results and discussion

2.1. Synthetic chemistry

The synthetic methods for the preparation **HBQ** derivatives **6a–d**, **9a–e** and **10a–e** obtained by structural modification at the C-23 and C-28 positions of **HBQ** are shown in Scheme 1, and the synthetic methods for the preparation **HBQ** analogues **18**, **21a–b** and **24a–b** based on ring-A substitutions are shown in Scheme 2.

The lead compound **HBQ** was obtained according to our

previous synthetic method [28]. Compounds **6a–d** were prepared by an amide reaction with different cyclic amines with NH moiety after deprotection of the C-28 carboxyl of **HBQ**. The C-28 carboxyl and C-23 hydroxyl of **HBQ** were reacted with ethyl bromoacetate and succinic anhydride, respectively, to obtain intermediates **8** and **3**, which were designed to reduce steric hindrance in the next modification with PEG. Intermediates **8** and **3** were reacted with PEG with different chain lengths in the presence of 4-dimethylaminopyridine (DMAP) and 1-(3-dimethylaminopropyl)-3-ethylcarbodiimide hydrochloride (EDCI) in anhydrous dichloromethane (DCM) to obtain target compounds **9a–e** and **10a–e**, respectively. In addition, using **HD** as the starting material, the C-28 carboxyl was protected by a benzyl group and the C-23 hydroxyl was protected by a *tert*-butyldimethylsilyl (TBDMS) group in turn, and then the C-3 hydroxyl was oxidized by pyridinium chlorochromate (PCC) to obtain intermediate **13**. Intermediate **13** was reacted with ethylenediamine in morpholine at 150 °C to furnish **14**. Compound **18** was synthesized by oxidation of intermediate **14** at the C-12 position with 30% H₂O₂ and deprotection of the C-23 hydroxyl. Intermediate **15** was substituted by bromine at the C-2 position and then reacted with thioacetamide in ethyl alcohol absolute at 95 °C to produce compound **21a**. Intermediate **15** was deprotected in the presence of Pd/C and then the methyl thiazole ring was fused to ring-A to produce compound **21b**. Intermediate **13** was reacted with ethyl formate under potassium *tert*-butanol catalysis to obtain intermediate **16**. Intermediate **16** was reacted with hydrazine hydrate in ethyl alcohol absolute in a heated reflux system to give intermediate **23**. Compounds **24a** and **24b** were prepared by deprotection of the C-23 hydroxyl and deprotection of the C-28 carboxyl of intermediate **23** in turn.

The NMR spectra of compounds **9a–e** and **10a–e** were similar to the lead compound **HBQ**, the proton signals of the PEG group in

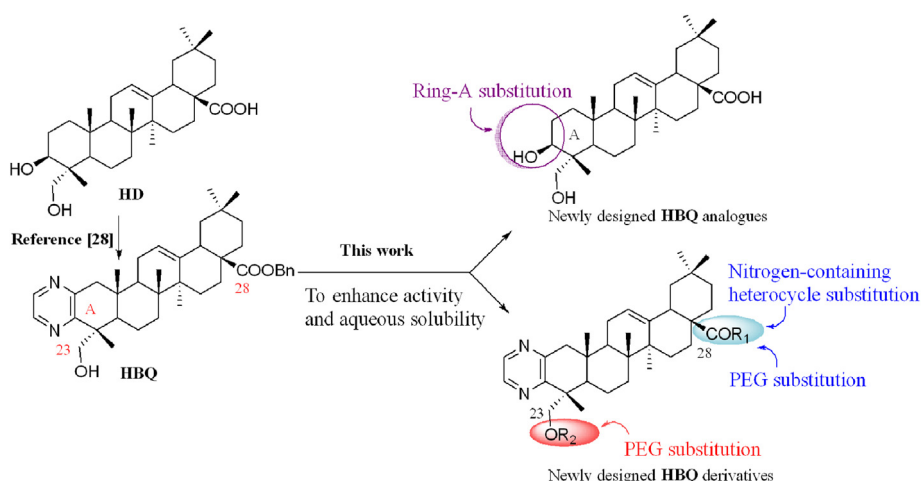
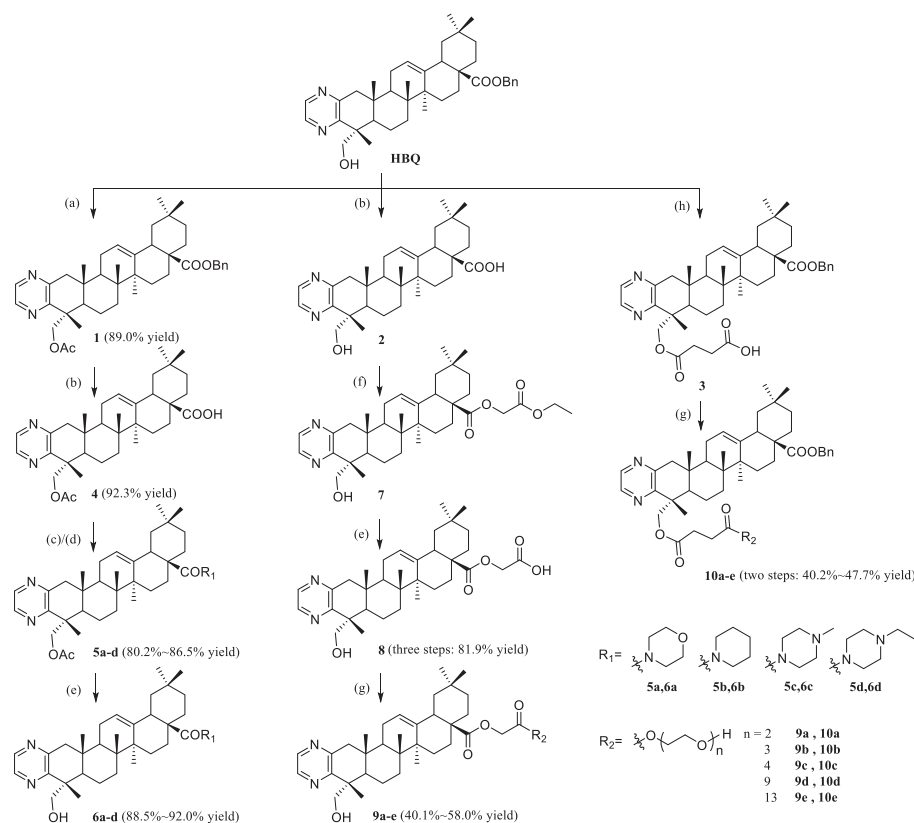
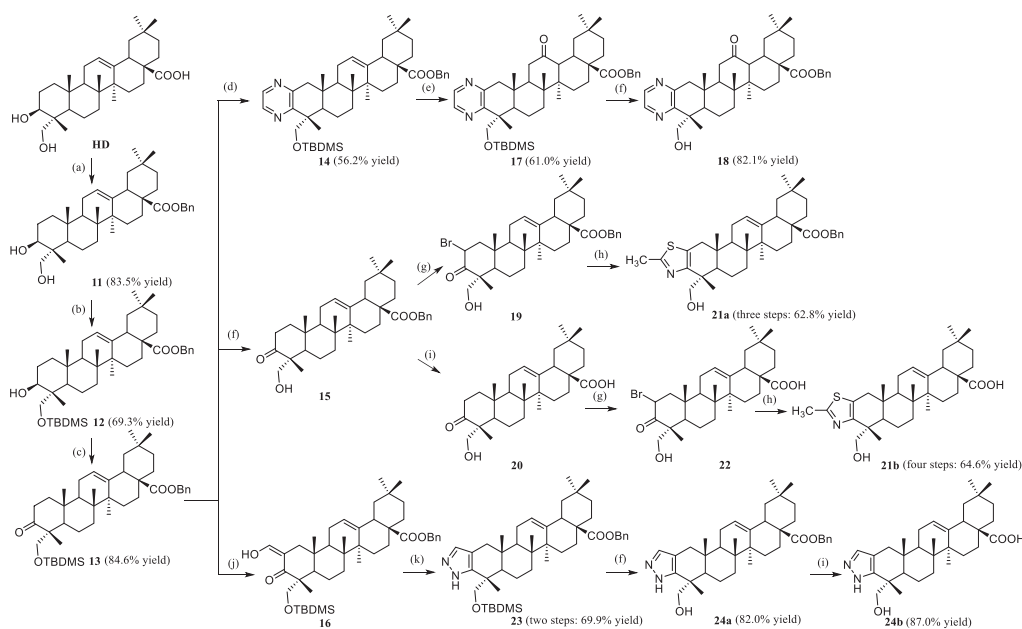


Fig. 4. The designed strategies for the HD derivatives.



Scheme 1. Synthesis of HD derivatives **6a-d**, **9a-e**, **10a-e**^{aa} Reagents and conditions: (a) Ac₂O, pyridine, r.t.; (b) 10% Pd/C, H₂, CH₃OH, r.t.; (c) (COCl)₂, DCM, 0 °C to r.t.; (d) cyclic amines with NH moiety, triethylamine, DCM, r.t.; (e) NaOH, CH₃OH/H₂O or CH₃OH/THF, r.t.; (f) ethyl bromoacetate, K₂CO₃, DMF, 65 °C; (g) PEG, DMAP, EDCI, DCM, r.t.; (h) succinic anhydride, DMAP, DCM, r.t.



Scheme 2. Synthesis of HD derivatives **18**, **21a-b**, **24a-b**^{bb} Reagents and conditions: (a) benzyl bromide, DMF, K₂CO₃, 50 °C; (b) tert-butyldimethylsilyl chloride, DMAP, DCM, r.t.; (c) PCC, DCM, r.t.; (d) S, ethylenediamine, morpholine, reflux; (e) 30% H₂O₂, HCO₂H, DCM, r.t.; (f) 10% HCl, acetone/CH₃OH, r.t.; (g) pyridinium bromide perbromide, CHCl₃, r.t.; (h) thioacetamide, ethyl alcohol absolute, 95 °C; (i) 10% Pd/C, H₂, CH₃OH, r.t.; (j) potassium t-butoxide, ethyl formate, DCM, r.t.; (k) hydrazine hydrate, EtOH, reflux.

each compound being the main difference. The ¹H NMR spectra of PEG had signals at δ 3.6–3.4 ppm from the protons of

—O—CH₂—CH₂— (the PEG chain) and the ¹³C NMR spectra had signals at δ 72–68 ppm from the carbons in the methylene groups.

The structures of all the **HD** derivatives were confirmed by ^1H NMR, ^{13}C NMR, and HR-MS.

2.2. Biological screening

The cytotoxicity and tumor MDR reversal activity toward KBV cells of the synthesized **HD** derivatives were investigated with the MTT assay [39], and the results are summarized in Table 1 and Fig. S1.

No compounds showed appreciable cytotoxicity at a concentration of 10 μM , which was reflected in the high survival rate of KBV cells in the absence of paclitaxel. Further, verapamil (a classic P-gp inhibitor) and compound **HBQ** were used as reference standards to evaluate the tumor MDR reversal activity of the synthesized compounds in combination with paclitaxel. Compounds **6a**, **6d**, **10c**, **10d**, and **10e** showed superior or equal activity compared with the lead compound **HBQ** at a concentration of 10 μM , displayed in bold font in Table 1. Among them, the lowest survival rate (11.97%) of KBV cells occurred when compound **10c** was combined with paclitaxel, which indicated that compound **10c** had the highest tumor MDR reversal activity. Moreover, compound **10c** increased the sensitivity of KBV cells to paclitaxel in a dose-dependent manner at concentrations of 2, 5 and 10 μM (Fig. S2). The above results showed that, as expected, **HBQ** derivatives with nitrogen-containing heterocycles or PEG modification could ameliorate the activity of **HBQ**. Most of the other derivatives also produced a lower survival rate for KBV cells when combined with paclitaxel, for example, the activity of compounds **6b**, **6c**, **9c**, **9d**, **18**, and **24a** was stronger than verapamil but weaker than **HBQ**.

2.3. Aqueous solubility determination of PEGylated derivatives

The poor aqueous solubility of **HBQ** is the major obstacle for further research. It is important to improve the aqueous solubility through specific structural modification methods while ensuring excellent activity. Therefore, we paid particular attention to the aqueous solubility of the most active derivative **10c** and the aqueous solubility of the series of PEGylated derivatives **10a–10e** was measured to explore the specific effects of PEGylation on the solubility. The aqueous solubility results are shown in Fig. 5(A).

As expected, compared with **HBQ**, the aqueous solubility of the PEGylated derivatives was significantly improved. The aqueous solubility of compound **10c** was $21.59 \pm 0.97 \mu\text{g/mL}$, which was approximately 20-fold higher than that of **HBQ** ($1.20 \pm 0.37 \mu\text{g/mL}$). Because of the strong solubilizing ability of PEG molecules with a large molecular weight, compounds **10d** and **10e** showed much higher solubility than **HBQ**, with values of 546.18 ± 6.49 and

$788.88 \pm 7.74 \mu\text{g/mL}$, respectively. The results showed that the aqueous solubility of compounds **10a–10e** was significantly improved by PEGylation, and the solubility increased with length of PEG chains, which may be because of the increase in hydrogen bond acceptors. Thus, PEGylation is an effective method to maintain activity and improve the aqueous solubility of compounds and the improved solubility of compound **10c** should enable further research and application of this compound.

2.4. In vitro stability of compound 10c

The excellent tumor resistance reversal activity *in vitro* and significantly improved aqueous solubility of compound **10c** indicated that the compound was worthy of further research. Therefore, we first investigated its stability *in vitro* to provide a basis for subsequent mechanism studies. The esterases in mammals are widely distributed in the plasma, organs, and tissues and play an indispensable role in drug metabolism. Porcine liver esterase (PLE), a widely accepted model of esterase activity [40,41], was selected to be added to PBS buffer (pH 7.4, 37 °C) to study the stability of compound **10c** in a simulated physiological environment. Meanwhile, benorylate [Fig. 5(C)], a recognized cleavable ester [42], was selected as a control to attest the viability of this test. The stability results are displayed in Fig. 5(B, D). Compound **10c** was highly stable under simulated physiological conditions as indicated by presence of $98.35 \pm 0.06\%$, $81.84 \pm 0.03\%$, and $78.92 \pm 0.03\%$ of the starting material following 4, 12, and 24 h of incubation, respectively. Compound **10c**, which is not a prodrug, possessed good chemical stability to an esterase and may remain stable in the circulation over 24 h, which would facilitate its stable transportation and tumor resistance reversal activity. Benorylate was hydrolyzed quickly under the same conditions, and only $14.10 \pm 0.23\%$ of the starting material existed after half an hour, which proved the viability of this stability determination method.

2.5. Effect of compound 10c on enhancing the sensitivity of KBV and MCF-7T cells toward paclitaxel and vincristine

The good solubility and stability of compound **10c** enlightened our in-depth activity evaluation and mechanism study. The effect of compound **10c** on the sensitivity of KBV and MCF-7T (paclitaxel-resistant breast carcinoma) cells toward paclitaxel and vincristine was investigated by MTT assay and compared with the lead **HBQ**, verapamil, and tariquidar (a third-generation P-gp inhibitor). The MDR reversal potency and reversal fold (RF) values of compound **10c** are summarized in Table 2.

Compound **10c** could significantly enhance the sensitivity of

Table 1
Effect of **HD** derivatives (10 μM) on the cytotoxicity of paclitaxel (100 nM) toward KBV cells^a.

Cpd. (10 μM)	KBV Cell Survival Rate (%)		Cpd. (10 μM)	KBV Cell Survival Rate (%)	
	With Paclitaxel (100 nM)	Without Paclitaxel		With Paclitaxel (100 nM)	Without Paclitaxel
Paclitaxel	103.48 \pm 2.88	–	9d	25.16 \pm 1.47	76.03 \pm 7.41
Verapamil	25.03 \pm 0.50	–	9e	39.13 \pm 2.53	73.26 \pm 6.01
HD	107.17 \pm 4.15	–	10a	79.47 \pm 6.19	72.66 \pm 9.42
HBQ	18.17 \pm 2.36	–	10b	43.54 \pm 0.95	82.53 \pm 2.94
HBQ-5	12.65 \pm 0.79	67.51 \pm 1.21	10c	11.97 \pm 0.06	90.29 \pm 13.37
6a	16.37 \pm 0.50	110.02 \pm 3.15	10d	15.38 \pm 2.42	70.58 \pm 2.71
6b	25.27 \pm 4.57	59.43 \pm 8.02	10e	15.93 \pm 0.32	69.69 \pm 2.69
6c	23.51 \pm 3.37	124.41 \pm 17.98	18	20.77 \pm 0.41	129.31 \pm 11.52
6d	16.67 \pm 1.27	120.48 \pm 16.62	21a	27.85 \pm 0.51	98.59 \pm 6.19
9a	26.15 \pm 0.63	81.65 \pm 1.54	21b	61.78 \pm 2.97	96.01 \pm 3.34
9b	28.76 \pm 1.00	80.47 \pm 0.97	24a	21.95 \pm 0.50	83.13 \pm 3.27
9c	25.88 \pm 0.43	75.43 \pm 4.31	24b	99.31 \pm 5.52	108.54 \pm 13.47

^a The cell survival rates are presented as the mean \pm SD of three independent experiments.

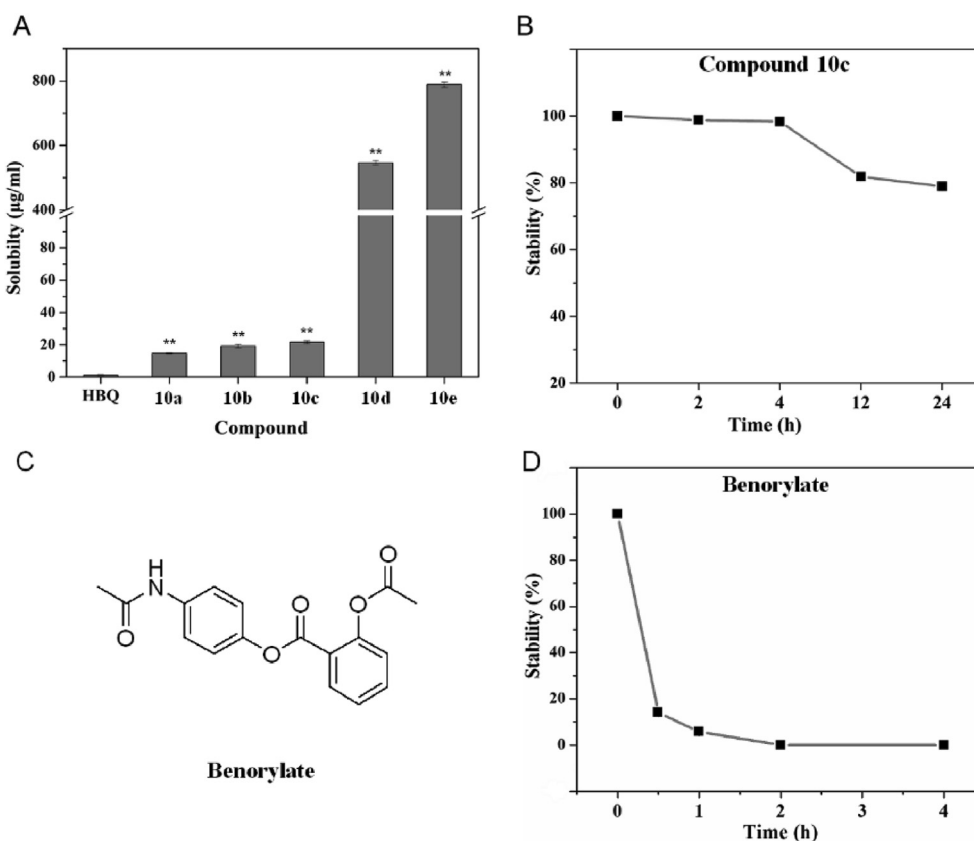


Fig. 5. (A) Aqueous solubility values of **HBQ** and the PEGylated derivatives **10a–10e** in deionized water at 37 °C. Data are represented as the mean \pm SD ($n = 3$). (B) *In vitro* stability of compound **10c** in the following environment: 0.01 M PBS at pH 7.4 with 20 units PLE ($n = 3$, mean \pm SD). (C) Chemical structure of benorylate. (D) *In vitro* stability of benorylate in the following environment: 0.01 M PBS at pH 7.4 with 57 units PLE ($n = 3$, mean \pm SD).

** $p < 0.01$, compared with **HBQ**.

Table 2

Effect of compound **10c**, **HBQ**, verapamil, and tariquidar on the cytotoxicity of paclitaxel and vincristine.

		KBV		MCF-7T	
		IC ₅₀ ^a (nM)	RF ^b	IC ₅₀ ^a (nM)	RF ^b
Paclitaxel (nM)	–	778.24 \pm 52.42	1.00	22.73 \pm 3.05	1.00
	+5 μ M 10c	21.84 \pm 2.13	35.63	5.42 \pm 0.23	4.19
	+10 μ M 10c	4.58 \pm 0.39**	169.96	0.89 \pm 0.24	25.50
	+5 μ M HBQ	59.17 \pm 6.49	13.15	12.99 \pm 1.95	1.75
	+10 μ M HBQ	15.80 \pm 2.10	49.25	1.48 \pm 0.51	15.40
	+5 μ M Verapamil	36.77 \pm 2.57	21.16	16.49 \pm 1.47	1.38
	+10 μ M Verapamil	23.08 \pm 2.01	33.72	8.51 \pm 1.83	2.67
	+5 μ M Tariquidar	7.57 \pm 0.52	102.80	3.26 \pm 1.26	6.97
	+10 μ M Tariquidar	4.46 \pm 0.35	174.60	0.26 \pm 0.12	86.28
	Vincristine (nM)	–	435.85 \pm 19.09	1.00	9.45 \pm 8.98
+5 μ M 10c		4.02 \pm 0.23	108.38	5.31 \pm 0.71	1.78
+10 μ M 10c		0.79 \pm 0.30**	550.59	0.04 \pm 0.03	269.55
+5 μ M HBQ		16.58 \pm 3.05	26.28	6.85 \pm 0.54	1.38
+10 μ M HBQ		2.23 \pm 0.10	195.27	0.03 \pm 0.02	309.98
+5 μ M Verapamil		4.59 \pm 0.10	94.86	10.17 \pm 0.98	0.93
+10 μ M Verapamil		2.97 \pm 0.24	146.72	5.29 \pm 1.23	1.79
+5 μ M Tariquidar		3.34 \pm 0.24	130.50	0.71 \pm 0.21	13.23
+10 μ M Tariquidar		2.05 \pm 0.21	212.45	0.22 \pm 0.15	43.35

** $p < 0.01$, compared with control group.

^a IC₅₀ values are represented as the mean \pm SD ($n = 3$).

^b RF value was calculated using the formula: RF = IC₅₀ of chemotherapeutic drug alone/IC₅₀ of chemotherapeutic drug in the presence of reversal agent.

KBV cells to the chemotherapeutic drugs paclitaxel and vincristine. Compound **10c** at a concentration of 10 μ M decreased the IC₅₀ values (4.58 and 0.79 nM when combined with paclitaxel and vincristine, respectively) and the RF values were as high as 169.96

and 550.59, respectively, compared with the chemotherapeutic drugs alone. The sensitization effect of compound **10c** on chemotherapeutic drugs was stronger than either the lead compound **HBQ** or the standard compound verapamil, and was almost

equivalent to tariquidar, and showed a dose-dependent effect at concentrations of 5 and 10 μM . Similarly, compound **10c** also enhanced the sensitivity of chemotherapy drugs to MCF-7T cells to varying degrees. These results indicated that compound **10c** could enhance the antitumor activity of chemotherapeutic drugs toward drug-resistant tumor cells.

2.6. Effect of compound **10c** on the efflux function of P-gp

Enhanced sensitivity of drug-resistant tumor cells to chemotherapeutic drugs may be achieved by increasing the accumulation of the chemotherapeutic drugs in the cells. Therefore, to investigate whether compound **10c** exerts a tumor resistance reversal effect by inhibiting the drug efflux function of P-gp, the effect on the efflux of rhodamine 123 and Flutax1 from KBV and MCF-7T cells was studied.

Rhodamine123 is a well-known P-gp substrate that is used as a biomarker to evaluate the effect of MDR reversal agents on the efflux function of P-gp [43]. It can be seen in Fig. 6(A and B) and

Figs. S3(A and B) that compound **10c** inhibited the P-gp-mediated efflux of rhodamine 123 in a dose-dependent manner, which was reflected in the increased accumulation of rhodamine 123 in KBV and MCF-7T cells. The effect was stronger than the positive controls **HBQ** and verapamil. Flutax1, a paclitaxel derivative that emits fluorescence upon binding to microtubules, is used as a P-gp substrate to characterize the function of P-gp [44]. As shown in Fig. 6(C and D) and Figs. S3(C and D), treatment with compound **10c** increased the accumulation of Flutax1 in KBV cells at a concentration of 5 μM and in MCF-7T cells at a concentration of 10 μM , thereby enhancing the antitumor effect of paclitaxel. The above results suggested that compound **10c** exerted a reversal effect on tumor MDR by effectively inhibiting the efflux function of P-gp.

2.7. Effect of compound **10c** on paclitaxel-induced cell cycle arrest and cell apoptosis in KBV cells

To investigate the effect of compound **10c** on paclitaxel-induced cell cycle arrest and apoptosis in KBV cells, the KBV cell cycle

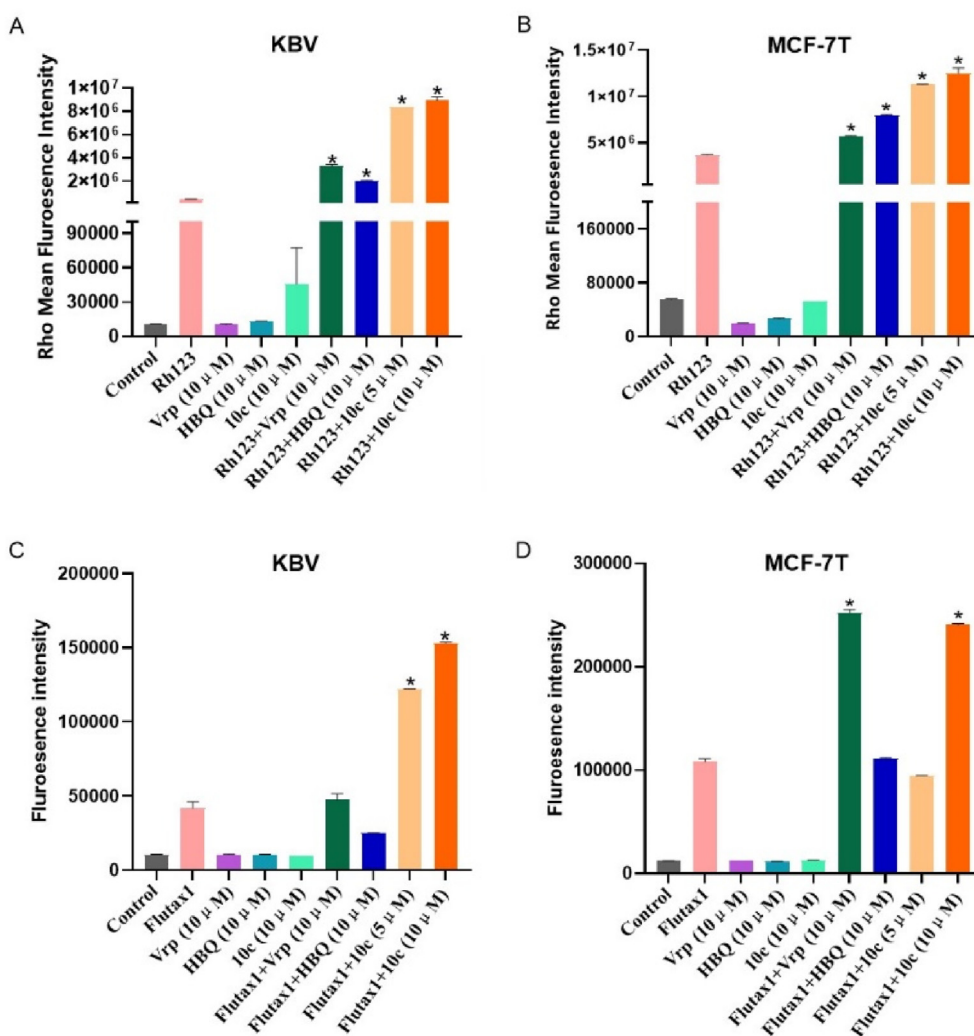


Fig. 6. Effect of compound **10c** on efflux function of P-gp in KBV and MCF-7T cells. (A) Effect of compound **10c** on the accumulation of rhodamine 123 in KBV cells. KBV cells were incubated with rhodamine 123 in the presence or absence of test compounds for 30 min for analysis by flow cytometry. (B) Effect of compound **10c** on the accumulation of rhodamine 123 in MCF-7T cells. MCF-7T cells were incubated with rhodamine 123 in the presence or absence of test compounds for 30 min for analysis by flow cytometry. (C) Effect of compound **10c** on the accumulation of Flutax1 in KBV cells. KBV cells were incubated with Flutax1 in the presence or absence of the test compounds for 30 min and then harvested for analysis by flow cytometry. (D) Effect of compound **10c** on the accumulation of Flutax1 in MCF-7T cells. MCF-7T cells were incubated with Flutax1 in the presence or absence of the test compounds for 30 min and then harvested for analysis by flow cytometry. All data are presented as the mean \pm SD ($n = 3$), * $p < 0.05$, compared with the Rh123 group (A, B) and Flutax1 group (C, D). Rh123: rhodamine 123; Vrp: verapamil.

distribution was analyzed by flow cytometry using propidium iodide (PI) staining. As shown in Fig. 7, compound **10c** significantly increased the rate of apoptosis in a dose-dependent manner. This effect was manifested as an increase in the proportion of KBV cells in the sub-G1 phase, which was increased from 2.1% to 48.9% after treatment with 10 μ M compound **10c** in combination with paclitaxel. However, compound **10c** had little effect on the paclitaxel-induced cell cycle arrest of the G2/M phase.

2.8. Molecular docking simulations

We used SYBYL software to conduct a molecular docking study to explore the specific influence of the structure of the synthesized compounds on their binding with P-gp. QZ-SSS with more drug-binding residues in a pair of stereoisomers in the literature [45,46] was selected as the reference molecule, and its binding pocket was used for molecular docking research. The docking scores of 19 compounds with a homology model of human P-gp are shown in Table 3. Most PEGylated derivatives showed higher docking scores than **HBQ**, except for compounds **9e** and **10e**. The docking positions of representative compounds **9d** and **10c** in the P-gp binding pocket are shown in Fig. 8(A and B). The oxygen atom of the carbonyl moiety of compound **9d** interacted with the amino

Table 3

Scores of the docking models of **HD** derivatives with a homology model of human P-gp.

Compound	Total_Score	Crash	Polar
Verapamil	6.6301	-1.9269	0.0907
HBQ	4.6288	-8.3403	1.0207
6a	4.2866	-10.4029	0.0006
6b	2.614	-11.1818	0.9548
6c	3.4525	-4.0402	1.0882
6d	2.8164	-7.7473	0.0001
9a	5.9506	-9.2299	1.1056
9b	5.3933	-10.4232	0.1304
9c	4.6424	-1.6426	1.9870
9d	9.0604	-6.1117	2.0635
9e	4.2427	-10.6122	2.7504
10a	5.9765	-12.8774	0.0061
10b	5.1472	-9.5701	0.9939
10c	7.0268	-6.1117	2.0635
10d	11.5472	-2.9517	1.4684
10e	4.3699	-11.9120	0.9938
18	4.0631	-5.2249	0.0007
21a	3.5854	-5.6353	1.0246
21b	0.8395	-7.4755	0
24a	2.7847	-9.0318	0
24b	2.0442	-7.5693	1.3406

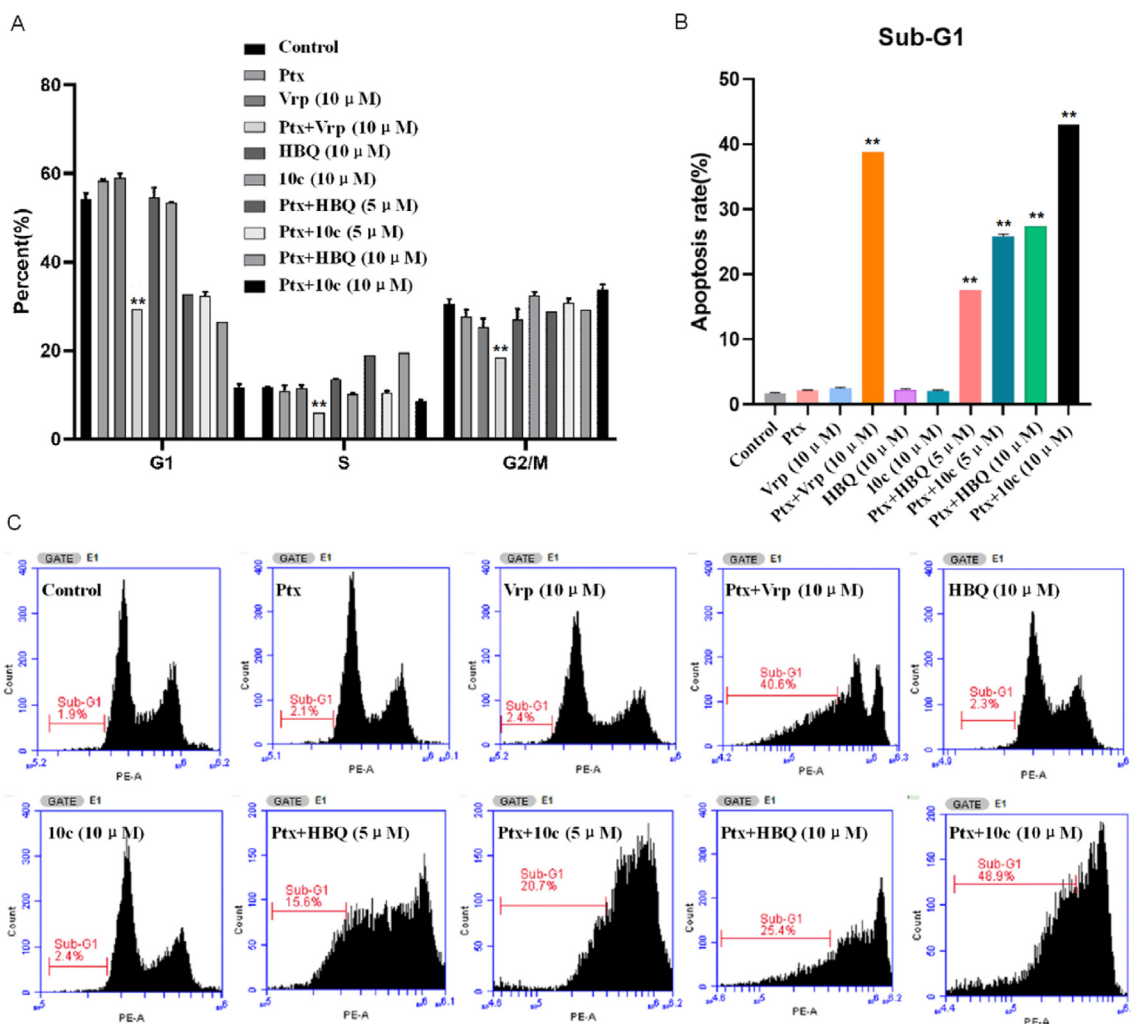


Fig. 7. Effect of **HBQ** and compound **10c** on paclitaxel activity in cell cycle distribution and apoptosis in KBV cells. (A): cell cycle distribution; (B): cell apoptosis; (C): **HBQ** and compound **10c** both enhanced paclitaxel-induced apoptosis, and compound **10c** demonstrated a greater ability to enhance cell apoptosis. All data are presented as the mean \pm SD ($n = 3$), ** $p < 0.01$, compared with control group. Ptx: paclitaxel; Vrp: verapamil.

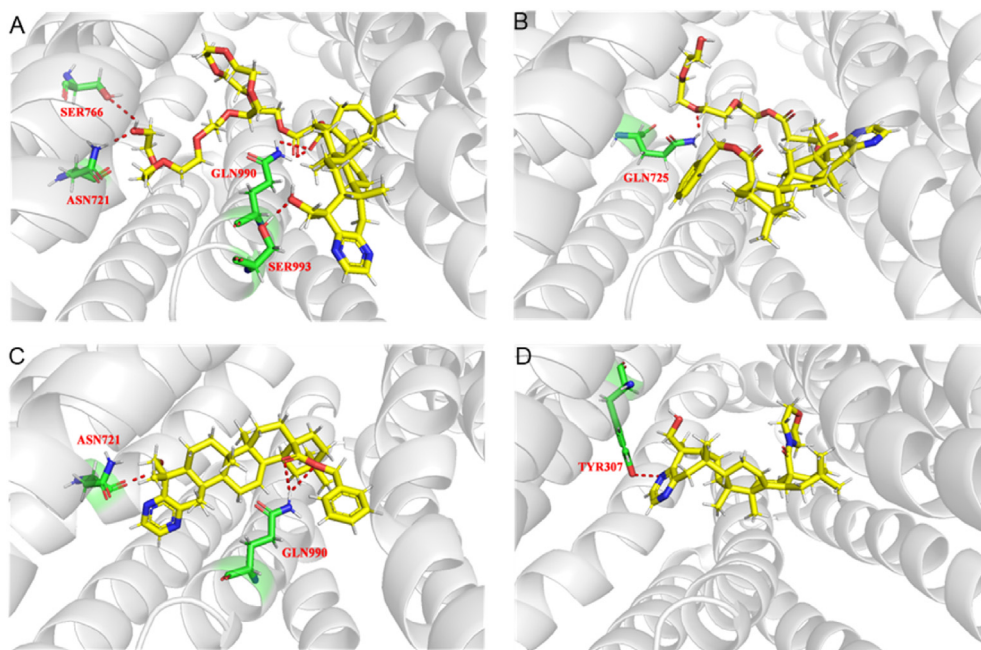


Fig. 8. Molecular docking mode of compounds **9d** (A), **10c** (B), **HBQ** (C), and **6a** (D) with a homology model of human P-gp. The compounds and amino acid residues are shown in stick format and hydrogen bonds are shown as dotted red lines. The figures were generated using PyMOL. (For interpretation of the colors in this figure, the reader is referred to the Web version of this article.)

acid residue GLN990 to form two hydrogen bonds (2.1 and 2.7 Å), which was similar to the binding interactions of **HBQ** [Fig. 8(C)]. In addition, the hydroxyl group at C-23 and the end of the PEG moiety were also bridged to SER993, ASN721, and SER766 by three hydrogen-bonding interactions, which further stabilized the binding in the pocket of P-gp. In contrast, the oxygen atom in the PEG side chain formed a hydrogen bond with the amino acid residue GLN725 in compound **10c**. However, through flexible changes in the docking position, compound **10c** could also be deeply embedded in the active pocket of P-gp. Amino acid residues GLN990, ASN721 and GLN725 mentioned above are identical to the binding residues of QZ-SSS. In addition, the derivatives **6a–d** with nitrogen-containing heterocycles substituted at C-28 had relatively low docking scores. For example, the docking position of compound **6a** [Fig. 8(D)] was closer to the top of the P-gp protein, and the compound did not penetrate as deeply as compound **10c** into the P-gp active pocket, which may be the reason why the activity of compound **6a** was lower than that of compound **10c**. In summary, these results indicated that PEGylated derivatives may reverse tumor MDR by acting on P-gp and that this docking method could provide direction for the future structural modification of **HD** derivatives with improved tumor MDR reversal activity.

2.9. Structure–activity relationships

According to the tumor MDR reversal activity evaluation of the synthesized **HD** derivatives and the SARs summarized in our previous study [29], the SARs were refined, as displayed in bold font in Fig. 9. When saturated nitrogen-containing heterocycles were substituted at C-28, activity was improved; however, open-chain nitrogen containing groups were better than the saturated nitrogen-containing heterocycles. When ring-A was a fused pyrazine and the C-28 carboxyl and the C-23 hydroxyl were substituted by PEG, activity was improved. When ring-A was a fused pyrazine and the double bond at C-12 was converted to a ketone, activity was improved. When ring-A was a fused

unsaturated nitrogen-containing heterocycle, activity was improved and the activity was further improved when the C-28 carboxyl was substituted by a benzyl group.

The tumor MDR reversal activity of compound **6d** was improved compared with compound **HBQ**, because of the *N*-ethyl piperazine substituted at C-28; however, it had less tumor MDR reversal activity than compound **HBQ-5** with 3-dimethylamino-1-propanol substituted at C-28, which indicated that open-chain nitrogen groups make a greater contribution to the activity than the *N*-ethyl piperazine group. Compounds **10c**, **10d**, and **10e** had higher tumor MDR reversal activity compared with compound **HBQ**, which is likely because of the introduction of PEG to increase the aqueous solubility. Compounds **21a** and **24a** displayed activity equal to verapamil at the same dose, and better activity than compounds **21b** and **24b**, respectively. These results show, under the premise that the C-28 carboxyl is protected by benzyl, that the activity is improved when ring-A is a fused unsaturated nitrogen-containing heterocycle. The existing SAR studies will be used to guide the design and synthesis of novel tumor MDR reversal agents with high activity, and more structural modifications of **HD** should continue to be carried out to further improve knowledge of the SAR.

3. Conclusions

In summary, we have designed and synthesized several series of nitrogen-containing heterocyclic-substituted, PEGylated, and ring-A substituted derivatives of hederagenin through amidation, esterification, and cyclization reactions, respectively. The MTT assay was used to evaluate the tumor MDR reversal activity of the derivatives as drug resistance reversal agents for tumor therapy. Almost all of the derivatives had a good reversal effect on drug-resistant KBV cells, with an effect stronger than, or equivalent to, verapamil. In addition, knowledge of the SARs of the **HD** derivatives were further improved. These structural modification methods will provide an important reference for the development of potential MDR reversal agents in the future. Notably, the aqueous solubility

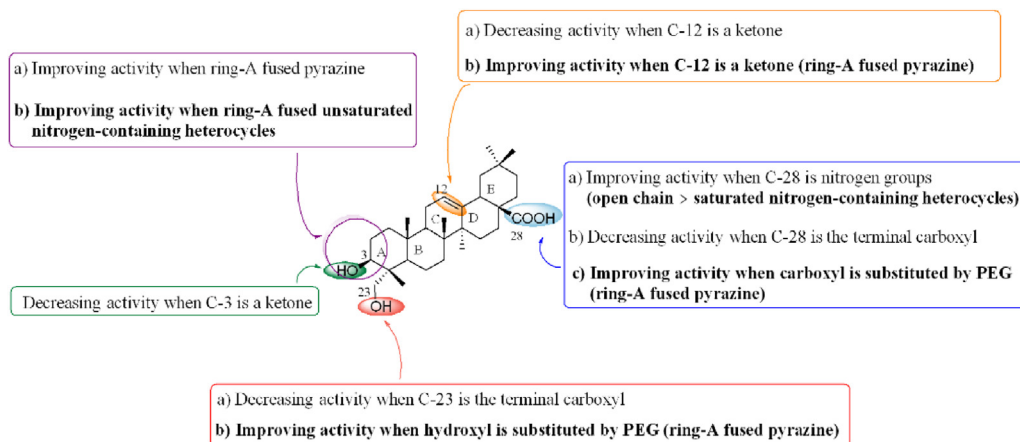


Fig. 9. Supplementary SARs of **HD** derivatives. The new SARs based on the results of this research are displayed in bold font.

of some of the PEGylated derivatives was 12–657 fold higher than the lead compound **HBQ**, and the aqueous solubility increased with length of PEG chains. Therefore, PEGylation is an effective method to improve aqueous solubility while maintaining tumor MDR reversal activity.

Compound **10c** was selected to evaluate the stability and the mechanism of the tumor MDR reversal effect. The results showed that compound **10c** possessed good chemical stability to an esterase over 24 h. Additionally, compound **10c** could significantly enhance the sensitivity of KBV cells to paclitaxel and vincristine, with IC_{50} values of 4.58 and 0.79 nM, respectively. The combination of compound **10c** and paclitaxel significantly increased the apoptosis rate of KBV cells. The results of flow cytometry showed that treatment with compound **10c** increased the accumulation of rhodamine 123 and Flutax1 in KBV and MCF-7T cells at concentrations of 5 and 10 μ M, which indicated that compound **10c** exerted the reversal of tumor resistance by effectively inhibiting the efflux function of P-gp. Moreover, compound **10c** showed a higher docking score than **HBQ** in the molecular docking study. Therefore, the above results strongly suggest that the *in vivo* activity, distribution, and metabolism of compound **10c** should be investigated, and these results will be published in due course.

4. Experimental section

4.1. Chemistry

All solvents and reagents were purchased from commercial sources, which were dried further by standard methods when necessary. All reactions were stirred magnetically, and the reaction progress was monitored by thin layer chromatography (TLC) analysis on silica gel HSGF254 and the spots visualized by using 10% ethanol sulfate solution and UV fluorescence with a wavelength of 254 nm. All the compounds we synthesized were purified by column chromatography on silica gel (200–300 mesh). ^1H (400 MHz) NMR spectra and ^{13}C (100 MHz) NMR spectra were recorded on Bruker av400 (Bruker, GER) or JNM-ECZ400S (JEOL Ltd., JPN) instrument in CDCl_3 , CD_3OD or $\text{DMSO-}d_6$ with TMS as internal standard. All chemical shifts were expressed in δ values parts per million (ppm) and the coupling constants (J) were given in Hertz (Hz). Took 1 mg each of all compounds and dissolved in DMSO, then diluted to 100 mg/mL with methanol to determine high resolution mass spectra (HR-MS). The HR-MS were taken on Agilent QTOF 6520 (Agilent Technologies Co. Ltd., USA), or Q ExactiveTM Orbitrap MS system (Thermo Scientific, USA). Melting points (m.p.) of all

solid compounds were tested using a Micro melting point determination apparatus SGW®X-4 (Shanghai INESA Physico-Optical Instrument Co., Ltd, CHN).

4.1.1. General procedure for the synthesis of **5a–5d**

The lead compound **HBQ** was obtained according to our previous synthetic method [28]. **HBQ** (2.0 g, 3.3 mmol) was dissolved in pyridine (30.0 mL) and acetic anhydride (15.9 mL) was added. The reaction was reacted with stirring at room temperature for 8 h. The mixture was diluted with ethyl acetate, washed with water and saturated brine in sequence, dried over Na_2SO_4 and concentrated. The residue was purified by silica gel column chromatography ($V_{\text{petroleum ether}}: V_{\text{ethyl acetate}} = 20:1$) to give a white solid **1** (1.5 g, 89.0% yield).

1 (1.9 g, 3.0 mmol) was dissolved in methanol (30.0 mL) and 10% Pd/C (0.6 g, 6.0 mmol) was added. The reaction was reacted with stirring under H_2 at room temperature for 6 h. The solution was collected by vacuum filtration. Then the mixture was concentrated and purified by silica gel column chromatography ($V_{\text{petroleum ether}}: V_{\text{ethyl acetate}} = 6:1$) to give a white solid **4** (1.5 g, 92.3% yield).

4 (90.0 mg, 0.2 mmol) was dissolved in anhydrous DCM (6 mL) with stirring for 10 min at 0 °C and then oxalyl chloride (160.0 μ L, 1.9 mmol) was added with stirring for 1 h. Remaining oxalyl chloride was removed by vacuum distillation, and the residue was dissolved in anhydrous DCM (6 mL) again, morpholine (160.0 μ L, 1.8 mmol) was added. The reaction was reacted with stirring at room temperature for 2 h. The mixture was diluted with ethyl acetate, washed with water and saturated brine in sequence, dried over Na_2SO_4 and concentrated. The residue was purified by silica gel column chromatography ($V_{\text{petroleum ether}}: V_{\text{ethyl acetate}} = 8:1$) to give a white solid **5a** (85.1 mg, 83.9% yield). The compounds **5b–5d** were made and purified with the same as synthesis of **5a**.

4.1.2. *N*-morpholine 23-hydroxy-olean[3,2-*b*]pyrazine-12-en-28-amide (**6a**)

5a (50 mg, 0.1 mmol) was dissolved in a component solvent ($V_{\text{tetrahydrofuran}}: V_{\text{methanol}} = 3:2$), and 10% sodium hydroxide solution (246.0 μ L) was dripped into the solution with stirring, reacted at room temperature for 5 h. The mixture was concentrated and then diluted with ethyl acetate. The solution was adjusted to acidic by using 5% hydrochloric acid solution. The organic phase was washed with water and saturated brine in sequence, dried over Na_2SO_4 , concentrated and purified by silica gel column chromatography ($V_{\text{petroleum ether}}: V_{\text{ethyl acetate}} = 8:1$) to give a white solid **6a** (42.1 mg, 90.3% yield). m.p. 147.1–149.3 °C. ^1H NMR (400 MHz, CDCl_3) δ 8.34

(d, $J = 8.0$ Hz, 2H, H-pyrazine), 5.34 (t, $J = 3.1$ Hz, 1H, H-12), 3.78 (d, $J = 10.6$ Hz, 1H, H-23a), 3.75–3.54 (m, 8H, 4 × NCH₂), 3.47 (d, $J = 10.6$ Hz, 1H, H-23b), 3.10 (d, $J = 11.2$ Hz, 1H, H-18), 2.99 (d, $J = 16.6$ Hz, 1H, H-1a), 2.49 (d, $J = 16.7$ Hz, 1H, H-1b), 1.30 (s, 3H, CH₃), 1.18 (s, 3H, CH₃), 0.93 (s, 6H, 2 × CH₃), 0.89 (s, 3H, CH₃), 0.83 (s, 3H, CH₃); ¹³C NMR (100 MHz, CDCl₃) δ 176.98, 159.36, 153.51, 146.03, 143.43, 143.00, 122.81, 71.98, 68.34, 61.79, 49.01, 48.86, 48.51, 47.70, 47.47, 47.28, 45.06, 44.75, 43.48, 40.44, 37.79, 35.38, 34.43, 33.43, 31.79, 31.29, 31.07, 29.34, 27.25, 25.43, 24.72, 24.10, 21.53, 20.77, 17.98, 17.49; HR-MS (ESI) m/z : calcd. for C₃₆H₅₃N₃O₃ [M+H]⁺: 576.4160, found: 576.4161.

4.1.3. *N*-piperidine 23-hydroxy-olean[3,2-*b*]pyrazine-12-en-28-amide (**6b**)

According to the synthesis method of **6a**, **5b** was deprotected to give a white solid **6b** (11.0 mg, 88.9% yield) after purified by silica gel column chromatography (V_{DCM}: V_{methanol} = 60:1). m.p. 145.2–149.6 °C. ¹H NMR (400 MHz, CDCl₃) δ 8.36 (q, $J = 2.4$ Hz, 2H, H-pyrazine), 5.35 (t, $J = 3.6$ Hz, 1H, H-12), 3.79 (d, $J = 10.6$ Hz, 1H, H-23a), 3.67–3.50 (m, 4H, 2 × NCH₂), 3.48 (d, $J = 10.5$ Hz, 1H, H-23b), 3.14 (dd, $J = 14.6, 3.0$ Hz, 1H, H-18), 3.01 (d, $J = 16.6$ Hz, 1H, H-1a), 2.50 (d, $J = 16.6$ Hz, 1H, H-1b), 1.33 (s, 3H, CH₃), 1.19 (s, 3H, CH₃), 0.95 (s, 3H, CH₃), 0.94 (s, 3H, CH₃), 0.90 (s, 3H, CH₃), 0.87 (s, 3H, CH₃); ¹³C NMR (100 MHz, CDCl₃) δ 174.79, 158.09, 152.25, 145.13, 142.13, 141.61, 121.19, 70.76, 53.50, 47.75, 47.51, 47.36, 46.69, 46.61, 46.04, 43.84, 43.38, 42.17, 39.12, 36.69, 34.21, 33.17, 32.18, 30.50, 29.85, 29.77, 28.11, 26.23, 25.90, 24.92, 24.18, 23.43, 22.76, 20.30, 19.43, 16.74, 16.20; HR-MS (ESI) m/z : calcd. for C₃₇H₅₅N₃O₂ [M+H]⁺: 574.4367, found: 574.4365.

4.1.4. *N*-(4'-methyl) piperazine 23-hydroxy-olean[3,2-*b*]pyrazine-12-en-28-amide (**6c**)

According to the synthesis method of **6a**, **5c** was deprotected to give a white solid **6c** (45.0 mg, 92.0% yield) after purified by silica gel column chromatography (V_{DCM}: V_{methanol} = 80:1). m.p. 138.5–144.2 °C. ¹H NMR (400 MHz, CDCl₃) δ 8.32 (d, $J = 8.4$ Hz, 2H, H-pyrazine), 5.32 (t, $J = 3.4$ Hz, 1H, H-12), 3.76 (d, $J = 10.5$ Hz, 1H, H-23a), 3.68–3.61 (m, 4H, 2 × NCH₂a), 3.46 (d, $J = 10.5$ Hz, 1H, H-23b), 3.09 (d, $J = 13.4$ Hz, 1H, H-18), 2.97 (d, $J = 16.6$ Hz, 1H, H-1a), 2.47 (d, $J = 16.6$ Hz, 1H, H-1b), 2.42–2.32 (m, 4H, 2 × NCH₂b), 2.29 (s, 3H, NCH₃), 1.29 (s, 3H, CH₃), 1.16 (s, 3H, CH₃), 0.91 (s, 6H, 2 × CH₃), 0.88 (s, 3H, CH₃), 0.81 (s, 3H, CH₃); ¹³C NMR (100 MHz, CDCl₃) δ 175.08, 158.00, 152.26, 144.84, 142.22, 141.63, 121.40, 70.71, 55.22, 47.78, 47.54, 47.27, 46.45, 45.99, 45.97, 45.23, 43.78, 43.40, 42.15, 39.13, 36.67, 34.12, 33.13, 32.15, 31.00, 30.48, 29.99, 29.34, 27.99, 25.92, 24.12, 23.41, 22.78, 20.28, 19.44, 16.71, 16.18; HR-MS (ESI) m/z : calcd. for C₃₇H₅₆N₄O₂ [M+H]⁺: 589.4476, found: 589.4470.

4.1.5. *N*-(4'-ethyl) piperazine 23-hydroxy-olean[3,2-*b*]pyrazine-12-en-28-amide (**6d**)

According to the synthesis method of **6a**, **5d** was deprotected to give a white solid **6d** (38.0 mg, 88.5% yield) after purified by silica gel column chromatography (V_{DCM}: V_{methanol} = 80:1). m.p. 133.5–139.1 °C. ¹H NMR (400 MHz, CDCl₃) δ 8.36 (d, $J = 2.5$ Hz, 1H, H-pyrazine), 8.34 (d, $J = 2.5$ Hz, 1H, H-pyrazine), 5.35 (t, $J = 3.5$ Hz, 1H, H-12), 3.80 (d, $J = 10.5$ Hz, 1H, H-23a), 3.71–3.63 (m, 4H, 2 × NCH₂a), 3.49 (d, $J = 10.5$ Hz, 1H, H-23b), 3.16–3.10 (m, 1H, H-18), 3.00 (d, $J = 16.6$ Hz, 1H, H-1a), 2.50 (d, $J = 16.7$ Hz, 1H, H-1b), 2.46–2.37 (m, 6H, 3 × NCH₂b), 1.32 (s, 3H, CH₃), 1.19 (s, 3H, CH₃), 1.10 (t, $J = 7.2$ Hz, 3H, CH₃), 0.94 (s, 6H, 2 × CH₃), 0.91 (s, 3H, CH₃), 0.85 (s, 3H, CH₃); ¹³C NMR (100 MHz, CDCl₃) δ 174.92, 157.93, 152.21, 144.81, 142.11, 141.56, 121.29, 70.59, 53.00, 52.29, 47.70, 47.44, 47.13, 46.38, 45.91, 45.26, 43.69, 43.36, 42.08, 39.05, 36.59, 34.05, 33.07, 32.08, 30.41, 29.91, 27.91, 25.86, 24.06, 23.34, 22.70, 20.19, 19.38, 16.66, 16.10, 11.87; HR-MS (ESI) m/z : calcd. for C₃₈H₅₈N₄O₂ [M+H]⁺:

603.4633, found: 603.4623.

4.1.6. General procedure for the synthesis of **8**

According to the synthesis method of **4**, **HBQ** was deprotected to give crude sodium **2**, which could be used directly for the next step without further purification.

Ethyl Bromoacetate (965.4 μ L, 8.7 mmol) and potassium carbonate (467.9 mg, 3.4 mmol) were added to a solution of **2** (816.0 mg, 1.6 mmol) in DMF (20 mL). The mixture was stirred for 3 h at 65 °C. Then the mixture was diluted with ethyl acetate, washed with water and saturated brine in sequence, dried over Na₂SO₄ and concentrated to give crude sodium **7**, which could be used directly for the next step without further purification.

7 (1023.0 mg, 1.7 mmol) was dissolved in a component solvent (V_{methanol}: V_{water} = 4:1), and sodium hydroxide (552.6 mg, 13.8 mmol) was added. The mixture was stirred for 1 h at room temperature. The mixture was concentrated and then diluted with ethyl acetate, washed with 5% hydrochloric acid solution, water and saturated brine in sequence, dried over Na₂SO₄ and concentrated. The residue was purified by silica gel column chromatography (V_{chloroform}: V_{methanol} = 100:1) to give a white solid **8** (879.7 mg, 81.9% yield).

4.1.7. *O*-(23-hydroxy-olean[3,2-*b*]pyrazine-12-en-28-acyl)-acetyldiethylene glycol (**9a**)

Diethylene glycol (108.0 μ L, 1.4 mmol), DMAP (150.1 mg, 1.2 mmol) and EDCI (148.8 mg, 0.8 mmol) were added to a solution of **8** (73 mg, 0.1 mmol) in dry DCM (5 mL). The mixture was stirred for 10 h at room temperature. Then the mixture was concentrated and dissolved in methanol, and the solution was dialyzed (MWCO 500 Da) in deionized water for 28 h and changed the dialysis liquid four times interval of 7 h. Dialysis substance was concentrated by vacuum distillation. The residue was purified by silica gel column chromatography (V_{DCM}: V_{methanol} = 185:1) to give a yellow transparent syrup **9a** (47.4 mg, 56.2% yield). ¹H NMR (400 MHz, CDCl₃) δ 8.37 (d, $J = 2.1$ Hz, 1H, H-pyrazine), 8.35 (d, $J = 2.5$ Hz, 1H, H-pyrazine), 5.38 (t, $J = 3.5$ Hz, 1H, H-12), 4.65 (d, $J = 15.8$ Hz, 1H, H-23a), 4.54 (d, $J = 15.8$ Hz, 1H, H-23b), 4.38–4.28 (m, 2H, CH₂O PEG group), 3.79 (d, $J = 10.6$ Hz, 1H, CH₂a), 3.75–3.57 (m, 6H, CH₂O PEG group), 3.49 (d, $J = 10.6$ Hz, 1H, CH₂b), 3.01 (d, $J = 16.6$ Hz, 1H, H-1a), 2.92 (d, $J = 13.2$ Hz, 1H, H-18), 2.51 (d, $J = 16.6$ Hz, 1H, H-1b), 1.33 (s, 3H, CH₃), 1.20 (s, 3H, CH₃), 0.95 (s, 6H, 2 × CH₃), 0.92 (s, 3H, CH₃), 0.83 (s, 3H, CH₃); ¹³C NMR (100 MHz, CDCl₃) δ 177.20, 168.02, 157.93, 152.09, 143.47, 142.14, 141.62, 122.35, 72.45, 70.65, 68.81, 64.01, 61.70, 60.45, 47.74, 47.15, 46.86, 45.97, 45.73, 43.33, 41.98, 41.36, 39.26, 36.53, 33.90, 33.05, 32.16, 31.91, 30.69, 27.60, 25.69, 23.60, 23.40, 23.11, 20.18, 19.40, 16.63, 16.14; HR-MS (ESI) m/z : calcd. for C₃₈H₅₆N₂O₇ [M+H]⁺: 653.4161, found: 653.4156.

4.1.8. *O*-(23-hydroxy-olean[3,2-*b*]pyrazine-12-en-28-acyl)-acetyltriethylene glycol (**9b**)

According to the synthesis method of **9a**, **8** was reacted with triethylene glycol to give a yellow transparent syrup **9b** (70.1 mg, 56.8% yield) after dialyzed (MWCO 500 Da) and purified by silica gel column chromatography (V_{DCM}: V_{methanol} = 135:1). ¹H NMR (400 MHz, CDCl₃) δ 8.37 (d, $J = 2.2$ Hz, 1H, H-pyrazine), 8.35 (d, $J = 2.5$ Hz, 1H, H-pyrazine), 5.38 (t, $J = 3.5$ Hz, 1H, H-12), 4.67 (d, $J = 15.8$ Hz, 1H, H-23a), 4.55 (d, $J = 15.8$ Hz, 1H, H-23b), 4.34–4.29 (m, 2H, CH₂O PEG group), 3.80 (d, $J = 10.6$ Hz, 1H, CH₂a), 3.72–3.59 (m, 10H, CH₂O PEG group), 3.49 (d, $J = 10.5$ Hz, 1H, CH₂b), 3.01 (d, $J = 16.6$ Hz, 1H, H-1a), 2.92 (dd, $J = 13.8, 4.1$ Hz, 1H, H-18), 2.51 (d, $J = 16.6$ Hz, 1H, H-1b), 1.33 (s, 3H, CH₃), 1.20 (s, 3H, CH₃), 0.95 (s, 6H, 2 × CH₃), 0.92 (s, 3H, CH₃), 0.83 (s, 3H, CH₃); ¹³C NMR (100 MHz, CDCl₃) δ 177.05, 168.03, 157.92, 152.09, 143.52, 142.14, 141.60, 122.31, 72.50, 70.65, 70.61, 70.31, 68.87, 64.07, 61.75, 60.33, 47.75, 47.16,

46.83, 45.90, 45.74, 43.33, 41.99, 41.37, 39.26, 36.53, 33.91, 33.05, 32.18, 31.90, 30.69, 27.59, 25.68, 23.60, 23.39, 23.12, 20.18, 19.39, 16.62, 16.13; HR-MS (ESI) m/z : calcd. for $C_{40}H_{60}N_2O_8$ $[M+H]^+$: 697.4423, found: 697.4420.

4.1.9. *O*-(23-hydroxy-olean[3,2-*b*]pyrazine-12-en-28-acyl)-acetyltetraethylene glycol (**9c**)

According to the synthesis method of **9a**, **8** was reacted with tetraethylene glycol to give a yellow transparent syrup **9c** (76.1 mg, 58.0% yield) after dialyzed (MWCO 500 Da) and purified by silica gel column chromatography ($V_{DCM}: V_{methanol} = 100:1$). 1H NMR (400 MHz, $CDCl_3$) δ 8.37 (s, 1H, H-pyrazine), 8.35 (s, 1H, H-pyrazine), 5.38 (t, $J = 3.4$ Hz, 1H, H-12), 4.66 (d, $J = 15.8$ Hz, 1H, H-23a), 4.55 (d, $J = 15.9$ Hz, 1H, H-23b), 4.33–4.28 (m, 2H, CH_2O PEG group), 3.79 (d, $J = 10.6$ Hz, 1H, CH_2a), 3.71–3.59 (m, 14H, CH_2O PEG group), 3.49 (d, $J = 10.6$ Hz, 1H, CH_2b), 3.01 (d, $J = 16.5$ Hz, 1H, H-1a), 2.92 (dd, $J = 13.8, 4.0$ Hz, 1H, H-18), 2.51 (d, $J = 16.6$ Hz, 1H, H-1b), 1.33 (s, 3H, CH_3), 1.19 (s, 3H, CH_3), 0.95 (s, 6H, $2 \times CH_3$), 0.92 (s, 3H, CH_3), 0.83 (s, 3H, CH_3); ^{13}C NMR (100 MHz, $CDCl_3$) δ 177.06, 168.07, 157.97, 152.15, 143.59, 142.19, 141.66, 122.35, 72.57, 70.70, 70.69, 70.62, 70.56, 70.38, 68.95, 64.22, 61.78, 60.38, 47.80, 47.19, 46.87, 45.94, 45.79, 43.39, 42.04, 41.41, 39.31, 36.58, 33.96, 33.09, 32.21, 31.95, 30.74, 27.65, 25.73, 23.66, 23.44, 23.17, 20.23, 19.45, 16.67, 16.18; HR-MS (ESI) m/z : calcd. for $C_{42}H_{64}N_2O_9$ $[M+H]^+$: 741.4685, found: 741.4682.

4.1.10. *O*-(23-hydroxy-olean[3,2-*b*]pyrazine-12-en-28-acyl)-acetylpolyethylene glycol 400 (**9d**)

According to the synthesis method of **9a**, **8** was reacted with polyethylene glycol 400 to give a yellow transparent syrup **9d** (68.3 mg, 40.1% yield) after dialyzed (MWCO 500 Da) and purified by silica gel column chromatography ($V_{DCM}: V_{methanol} = 80:1$). 1H NMR (400 MHz, $CDCl_3$) δ 8.38 (d, $J = 2.1$ Hz, 1H, H-pyrazine), 8.35 (d, $J = 2.4$ Hz, 1H, H-pyrazine), 5.38 (t, $J = 3.5$ Hz, 1H, H-12), 4.66 (d, $J = 15.8$ Hz, 1H, H-23a), 4.54 (d, $J = 15.8$ Hz, 1H, H-23b), 4.32–4.27 (m, 2H, CH_2O PEG group), 3.80 (d, $J = 10.6$ Hz, 1H, CH_2a), 3.74–3.57 (m, 32H, CH_2O PEG group), 3.49 (d, $J = 10.6$ Hz, 1H, CH_2b), 3.01 (d, $J = 16.6$ Hz, 1H, H-1a), 2.91 (dd, $J = 14.3, 3.4$ Hz, 1H, H-18), 2.51 (d, $J = 16.6$ Hz, 1H, H-1b), 1.33 (s, 3H, CH_3), 1.20 (s, 3H, CH_3), 0.95 (s, 6H, $2 \times CH_3$), 0.92 (s, 3H, CH_3), 0.83 (s, 3H, CH_3); ^{13}C NMR (100 MHz, $CDCl_3$) δ 176.99, 168.01, 152.07, 143.55, 142.11, 141.63, 122.28, 99.93, 72.62, 70.68–70.24, 68.88, 64.23, 61.67, 60.34, 47.72, 47.17, 46.83, 45.91, 45.75, 43.33, 41.99, 41.38, 39.26, 36.54, 33.92, 33.06, 32.19, 31.92, 30.70, 27.60, 25.68, 23.62, 23.40, 23.13, 20.18, 19.40, 16.63, 16.15; HR-MS (ESI) m/z : calcd. for $C_{52}H_{84}N_2O_{14}$ $[M+H]^+$: 961.5996, found: 961.5984.

4.1.11. *O*-(23-hydroxy-olean[3,2-*b*]pyrazine-12-en-28-acyl)-acetylpolyethylene glycol 600 (**9e**)

According to the synthesis method of **9a**, **8** was reacted with polyethylene glycol 600 to give a yellow transparent syrup **9e** (106.5 mg, 45.2% yield) after dialyzed (MWCO 1000 Da) and purified by silica gel column chromatography ($V_{DCM}: V_{methanol} = 75:1$). 1H NMR (400 MHz, $CDCl_3$) δ 8.38 (s, 2H, H-pyrazine), 5.38 (t, $J = 3.5$ Hz, 1H, H-12), 4.66 (d, $J = 15.8$ Hz, 1H, H-23a), 4.54 (d, $J = 15.8$ Hz, 1H, H-23b), 4.31–4.29 (m, 2H, CH_2O PEG group), 3.80 (d, $J = 10.4$ Hz, 1H, CH_2a), 3.74–3.59 (m, 50H, CH_2O PEG group), 3.49 (d, $J = 10.5$ Hz, 1H, CH_2b), 3.01 (d, $J = 17.1$ Hz, 1H, H-1a), 2.92 (dd, $J = 13.5, 4.3$ Hz, 1H, H-18), 2.51 (d, $J = 15.0$ Hz, 1H, H-1b), 1.33 (s, 3H, CH_3), 1.20 (s, 3H, CH_3), 0.95 (s, 6H, $2 \times CH_3$), 0.92 (s, 3H, CH_3), 0.83 (s, 3H, CH_3); ^{13}C NMR (100 MHz, $CDCl_3$) δ 176.99, 168.00, 152.08, 143.54, 142.08, 141.66, 122.29, 72.67, 70.76–70.24, 68.87, 64.22, 61.66, 60.33, 47.73, 47.13, 46.82, 45.91, 45.74, 43.35, 41.99, 41.37, 39.26, 36.53, 33.91, 33.05, 32.17, 31.90, 30.69, 27.60, 25.68, 23.61, 23.40, 23.12, 20.18, 19.40, 16.62, 16.14; HR-MS (ESI) m/z : calcd. for

$C_{60}H_{100}N_2O_{18}$ $[M+H]^+$: 1137.7044, found: 1137.7046.

4.1.12. General procedure for the synthesis of **3**

To a solution of **HBQ** (443 mg, 0.7 mmol) in anhydrous DCM (25 mL) was added succinic anhydride (742.8 mg, 7.4 mmol) and DMAP (453.4 mg, 3.7 mmol). After stirring for 2 h at room temperature, the mixture was diluted with DCM, washed with water and saturated brine in sequence, dried over Na_2SO_4 and concentrated to give crude sodium **3**, which could be used directly for the next step without further purification.

4.1.13. 4-(Benzyl olean[3,2-*b*]pyrazine-12-en-28-oate-23-oxy)-4-oxo-butyryldiethylene glycol (**10a**)

Diethylene glycol (101.7 μ L, 1.2 mmol) was dissolved in anhydrous DCM (8 mL), and **3** (90 mg, 0.1 mmol), DMAP (149.9 mg, 1.2 mmol), EDCl (148.5 mg, 0.8 mmol) were added in turn. The mixture was stirred for 10 h at room temperature. Then the mixture was concentrated and dissolved in methanol, and the solution was dialyzed (MWCO 500 Da) in deionized water for 28 h and changed the dialysis liquid four times interval of 7 h. Dialysis substance was concentrated by vacuum distillation. The residue was purified by silica gel column chromatography ($V_{DCM}: V_{methanol} = 250:1$) to give a yellow transparent syrup **10a** (47.0 mg, 45.8% yield). 1H NMR (400 MHz, $CDCl_3$) δ 8.42 (s, 1H, H-pyrazine), 8.29 (s, 1H, H-pyrazine), 7.38–7.28 (m, 5H, $5 \times H-Ar$), 5.37 (t, $J = 3.5$ Hz, 1H, H-12), 5.14–5.03 (m, 2H, CH_2Ar), 4.32 (d, $J = 10.5$ Hz, 1H, H-23a), 4.27 (d, $J = 10.5$ Hz, 1H, H-23b), 4.20–4.16 (m, 2H, CH_2O PEG group), 3.77–3.57 (m, 6H, CH_2O PEG group), 2.99–2.93 (m, 2H, H-1a, H-18), 2.51 (d, $J = 16.3$ Hz, 1H, H-1b), 2.46–2.33 (m, 4H, $2 \times CH_2$), 1.28 (s, 3H, CH_3), 1.19 (s, 3H, CH_3), 0.94 (s, 3H, CH_3), 0.91 (s, 3H, CH_3), 0.88 (s, 3H, CH_3), 0.69 (s, 3H, CH_3); ^{13}C NMR (100 MHz, $CDCl_3$) δ 177.43, 171.91, 171.82, 156.19, 152.31, 143.72, 142.39, 141.65, 136.41, 128.43, 128.03, 127.94, 122.29, 72.53, 71.01, 68.93, 65.97, 63.72, 61.71, 47.66, 46.81, 46.11, 45.85, 45.66, 43.18, 41.91, 41.56, 39.20, 36.58, 33.89, 33.10, 32.35, 31.82, 30.72, 29.70, 29.32, 29.02, 28.81, 27.63, 25.75, 23.61, 23.35, 23.10, 19.85, 19.79, 16.64, 15.74; HR-MS (ESI) m/z : calcd. for $C_{47}H_{64}N_2O_8$ $[M+H]^+$: 785.4735, found: 785.4723.

4.1.14. 4-(Benzyl olean[3,2-*b*]pyrazine-12-en-28-oate-23-oxy)-4-oxo-butyryltriethylene glycol (**10b**)

According to the synthesis method of **10a**, **3** was reacted with triethylene glycol to give a yellow transparent syrup **10b** (46.0 mg, 47.7% yield) after dialyzed (MWCO 500 Da) and purified by silica gel column chromatography ($V_{DCM}: V_{methanol} = 150:1$). 1H NMR (400 MHz, $CDCl_3$) δ 8.42 (d, $J = 2.1$ Hz, 1H, H-pyrazine), 8.29 (d, $J = 2.3$ Hz, 1H, H-pyrazine), 7.37–7.28 (m, 5H, $5 \times H-Ar$), 5.37 (t, $J = 3.4$ Hz, 1H, H-12), 5.13–5.04 (m, 2H, CH_2Ar), 4.32 (d, $J = 10.5$ Hz, 1H, H-23a), 4.27 (d, $J = 10.5$ Hz, 1H, H-23b), 4.21–4.15 (m, 2H, CH_2O PEG group), 3.74–3.59 (m, 10H, CH_2O PEG group), 3.02–2.90 (m, 2H, H-1a, H-18), 2.52 (d, $J = 13.8$ Hz, 1H, H-1b), 2.49–2.31 (m, 4H, $2 \times CH_2$), 1.27 (s, 3H, CH_3), 1.19 (s, 3H, CH_3), 0.94 (s, 3H, CH_3), 0.91 (s, 3H, CH_3), 0.88 (s, 3H, CH_3), 0.69 (s, 3H, CH_3); ^{13}C NMR (100 MHz, $CDCl_3$) δ 177.43, 171.97, 171.89, 156.15, 152.34, 143.70, 142.38, 141.73, 136.41, 128.43, 128.02, 127.94, 122.30, 72.53, 70.98, 70.58, 70.34, 69.02, 65.97, 63.67, 61.74, 47.67, 46.81, 46.14, 45.85, 45.65, 43.19, 41.91, 41.55, 39.19, 36.58, 33.89, 33.10, 32.35, 31.82, 30.72, 29.69, 29.36, 28.94, 28.79, 27.62, 25.75, 23.61, 23.35, 23.10, 19.86, 19.79, 16.64, 15.73; HR-MS (ESI) m/z : calcd. for $C_{49}H_{68}N_2O_9$ $[M+H]^+$: 829.4998, found: 829.4988.

4.1.15. 4-(Benzyl olean[3,2-*b*]pyrazine-12-en-28-oate-23-oxy)-4-oxo-butyryltetraethylene glycol (**10c**)

According to the synthesis method of **10a**, **3** was reacted with tetraethylene glycol to give a yellow transparent syrup **10c** (46.3 mg, 45.6% yield) after dialyzed (MWCO 500 Da) and purified

by silica gel column chromatography ($V_{\text{DCM}}: V_{\text{methanol}} = 150:1$). ^1H NMR (400 MHz, CDCl_3) δ 8.41 (d, $J = 2.4$ Hz, 1H, H-pyrazine), 8.29 (d, $J = 2.5$ Hz, 1H, H-pyrazine), 7.36–7.30 (m, 5H, $5 \times \text{H-Ar}$), 5.37 (t, $J = 3.5$ Hz, 1H, H-12), 5.13–5.04 (m, 2H, CH_2Ar), 4.32 (d, $J = 10.5$ Hz, 1H, H-23a), 4.27 (d, $J = 10.5$ Hz, 1H, H-23b), 4.21–4.16 (m, 2H, CH_2O PEG group), 3.74–3.59 (m, 14H, CH_2O PEG group), 2.99–2.93 (m, 2H, H-1a, H-18), 2.54 (d, $J = 16.4$ Hz, 1H, H-1b), 2.49–2.34 (m, 4H, $2 \times \text{CH}_2$), 1.27 (s, 3H, CH_3), 1.19 (s, 3H, CH_3), 0.94 (s, 3H, CH_3), 0.91 (s, 3H, CH_3), 0.88 (s, 3H, CH_3), 0.69 (s, 3H, CH_3); ^{13}C NMR (100 MHz, CDCl_3) δ 177.44, 171.99, 171.92, 156.19, 152.31, 143.70, 142.41, 141.69, 136.41, 128.43, 128.02, 127.94, 122.30, 72.57, 70.97, 70.64, 70.55, 70.53, 70.33, 69.06, 65.97, 63.77, 61.74, 47.65, 46.82, 46.14, 45.85, 45.66, 43.20, 41.91, 41.56, 39.20, 36.58, 33.90, 33.10, 32.36, 31.82, 30.73, 29.70, 28.93, 28.79, 27.63, 27.42, 25.76, 23.62, 23.36, 23.11, 19.86, 19.80, 16.65, 15.74; HR-MS (ESI) m/z : calcd. for $\text{C}_{51}\text{H}_{72}\text{N}_2\text{O}_{10}$ $[\text{M}+\text{H}]^+$: 873.5260, found: 873.5223.

4.1.16. 4-(Benzyl olean[3,2-*b*]pyrazine-12-en-28-oate-23-oxy)-4-oxo-butyrylpolyethylene glycol 400 (**10d**)

According to the synthesis method of **10a**, **3** was reacted with polyethylene glycol 400 to give a yellow transparent syrup **10d** (76.8 mg, 40.2% yield) after dialyzed (MWCO 500 Da) and purified by silica gel column chromatography ($V_{\text{DCM}}: V_{\text{methanol}} = 80:1$). ^1H NMR (400 MHz, CDCl_3) δ 8.41 (d, $J = 2.2$ Hz, 1H, H-pyrazine), 8.29 (d, $J = 2.3$ Hz, 1H, H-pyrazine), 7.37–7.29 (m, 5H, $5 \times \text{H-Ar}$), 5.38 (t, $J = 3.5$ Hz, 1H, H-12), 5.12–5.04 (m, 2H, CH_2Ar), 4.33 (d, $J = 10.5$ Hz, 1H, H-23a), 4.27 (d, $J = 10.5$ Hz, 1H, H-23b), 4.20–4.14 (m, 2H, CH_2O PEG group), 3.73–3.60 (m, 32H, CH_2O PEG group), 2.98–2.93 (m, 2H, H-1a, H-18), 2.51 (d, $J = 16.9$ Hz, 1H, H-1b), 2.54–2.45 (m, 4H, $2 \times \text{CH}_2$), 1.27 (s, 3H, CH_3), 1.19 (s, 3H, CH_3), 0.94 (s, 3H, CH_3), 0.91 (s, 3H, CH_3), 0.88 (s, 3H, CH_3), 0.69 (s, 3H, CH_3); ^{13}C NMR (100 MHz, CDCl_3) δ 177.43, 171.97, 171.89, 156.10, 152.36, 143.70, 142.36, 141.78, 136.40, 128.43, 128.02, 127.94, 122.30, 72.63, 70.97–70.27, 69.03, 65.96, 63.80, 61.69, 47.71, 46.81, 46.14, 45.84, 45.65, 43.18, 41.90, 41.55, 39.19, 36.58, 33.89, 33.10, 32.35, 31.82, 30.72, 29.69, 28.98, 28.90, 28.78, 27.62, 25.75, 23.61, 23.34, 23.10, 19.86, 19.80, 16.64, 15.73; HR-MS (ESI) m/z : calcd. for $\text{C}_{61}\text{H}_{92}\text{N}_2\text{O}_{15}$ $[\text{M}+\text{H}]^+$: 1093.6571, found: 1093.6556.

4.1.17. 4-(Benzyl olean[3,2-*b*]pyrazine-12-en-28-oate-23-oxy)-4-oxo-butyrylpolyethylene glycol 600 (**10e**)

According to the synthesis method of **10a**, **3** was reacted with polyethylene glycol 600 to give a yellow transparent syrup **10e** (68.8 mg, 41.4% yield) after dialyzed (MWCO 1000 Da) and purified by silica gel column chromatography ($V_{\text{DCM}}: V_{\text{methanol}} = 60:1$). ^1H NMR (400 MHz, CDCl_3) δ 8.41 (d, $J = 2.3$ Hz, 1H, H-pyrazine), 8.29 (d, $J = 2.4$ Hz, 1H, H-pyrazine), 7.37–7.31 (m, 5H, $5 \times \text{H-Ar}$), 5.38 (t, $J = 3.5$ Hz, 1H, H-12), 5.13–5.04 (m, 2H, CH_2Ar), 4.33 (d, $J = 10.5$ Hz, 1H, H-23a), 4.27 (d, $J = 10.5$ Hz, 1H, H-23b), 4.19–4.15 (m, 2H, CH_2O PEG group), 3.73–3.60 (m, 50H, CH_2O PEG group), 2.99–2.93 (m, 2H, H-1a, H-18), 2.52 (d, $J = 16.5$ Hz, 1H, H-1b), 2.50–2.32 (m, 4H, $2 \times \text{CH}_2$), 1.27 (s, 3H, CH_3), 1.19 (s, 3H, CH_3), 0.94 (s, 3H, CH_3), 0.91 (s, 3H, CH_3), 0.88 (s, 3H, CH_3), 0.69 (s, 3H, CH_3); ^{13}C NMR (100 MHz, CDCl_3) δ 177.44, 171.98, 171.89, 156.14, 152.34, 143.70, 142.38, 141.74, 136.41, 128.43, 128.02, 127.94, 122.30, 72.64, 70.97–70.28, 69.03, 65.96, 63.80, 61.70, 47.69, 46.81, 46.14, 45.84, 45.65, 43.19, 41.90, 41.55, 39.19, 36.58, 33.90, 33.10, 32.35, 31.82, 30.72, 29.69, 28.91, 28.78, 27.62, 25.76, 23.61, 23.35, 23.11, 19.86, 19.80, 18.43, 16.64, 15.73; HR-MS (ESI) m/z : calcd. for $\text{C}_{69}\text{H}_{108}\text{N}_2\text{O}_{19}$ $[\text{M}+\text{H}]^+$: 1269.7619, found: 1269.7604.

4.1.18. General procedure for the synthesis of **13**

The synthesis of the key intermediate **13** used **HD** as the starting compound with three steps of protection of C-28 carboxyl, protection of C-23 hydroxyl, oxidation of C-3 hydroxyl, according to the

previous experimental method [24].

4.1.19. General procedure for the synthesis of **17**

13 (7.3 g, 10.8 mmol) and sulphur (10.4 mg, 324.3 mmol) were dissolved in dry morpholine (250.0 mL) and ethylene diamine (14.4 mL, 215.6 mmol) was added. The reaction was refluxed at 150 °C for 2 h. The mixture was diluted with ethyl acetate, washed with water and saturated brine in sequence, dried over Na_2SO_4 and concentrated. The residue was purified by silica gel column chromatography ($V_{\text{petroleum ether}}: V_{\text{ethyl acetate}} = 25:1$) to give a white solid **14** (4.3 g, 56.2% yield).

To a solution of **14** (90.0 mg, 0.1 mmol) in anhydrous DCM (6 mL) was added methanoic acid (312.0 μL) and 30% H_2O_2 (128 μL), the reaction was reacted with stirring at room temperature for 28 h. The reaction solution was washed to neutral with saturated sodium bicarbonate solution and washed twice with saturated brine, dried over Na_2SO_4 and concentrated. The residue was purified by silica gel column chromatography ($V_{\text{petroleum ether}}: V_{\text{ethyl acetate}} = 8:1$) to give a white solid **17** (72.8 mg, 61.0% yield).

4.1.20. Benzyl 23-hydroxy-olean[3,2-*b*]pyrazine-12-oxo-28-oate (**18**)

17 (60 mg, 0.1 mmol) was dissolved in acetone (5 mL) and 10% hydrochloric acid solution (282.0 μL) was added with stirring for 10 h at room temperature. The mixture was diluted with ethyl acetate, washed with water to neutral and then washed with saturated brine, dried over Na_2SO_4 and concentrated. The residue was purified by silica gel column chromatography ($V_{\text{petroleum ether}}: V_{\text{ethyl acetate}} = 6:1$) to give a white solid **18** (41.5 mg, 82.1%). m.p. 159.6–161.9 °C. ^1H NMR (400 MHz, CDCl_3) δ 8.29 (d, $J = 3.9$ Hz, 1H, H-pyrazine), 8.02 (d, $J = 4.0$ Hz, 1H, H-pyrazine), 7.39–7.30 (m, 5H, $5 \times \text{H-Ar}$), 5.21, 5.09 (each 1H, d, $J = 12.2$ Hz, 1H, CH_2Ar), 3.80 (d, $J = 10.7$ Hz, 1H, H-23a), 3.46 (d, $J = 10.7$ Hz, 1H, H-23b), 3.24 (d, $J = 18.2$ Hz, 1H, H-13), 2.85 (dd, $J = 13.4, 3.2$ Hz, 1H, H-1a), 2.51 (d, $J = 4.2$ Hz, 1H, H-18), 2.45 (dd, $J = 16.3, 4.5$ Hz, 1H, H-1b), 1.32 (s, 3H, CH_3), 1.01 (s, 3H, CH_3), 0.95 (s, 3H, CH_3), 0.92 (s, 3H, CH_3), 0.81 (s, 3H, CH_3), 0.68 (s, 3H, CH_3); ^{13}C NMR (100 MHz, CDCl_3) δ 210.24, 177.39, 161.44, 143.30, 142.61, 136.23, 131.48, 128.44, 128.12, 69.81, 65.92, 53.39, 51.68, 48.31, 47.10, 45.16, 44.04, 42.08, 40.97, 38.35, 37.96, 36.14, 35.40, 34.38, 33.32, 32.73, 31.98, 30.62, 30.30, 27.28, 25.59, 23.08, 22.58, 20.31, 19.70, 18.72, 16.36, 15.05; HR-MS (ESI) m/z : calcd. for $\text{C}_{39}\text{H}_{52}\text{N}_2\text{O}_4$ $[\text{M}+\text{H}]^+$: 613.4000, found: 613.3998.

4.1.21. General procedure for the synthesis of **19**

According to the synthesis method of **18**, **13** was deprotected to give crude sodium **15**, which could be used directly for the next step without further purification.

15 (458.0 mg, 0.8 mmol) was dissolved in chloroform (50.0 mL) and pyridinium bromide perbromide (259.0 mg, 0.8 mmol) was added with stirring for 4 h at room temperature. The mixture was diluted with DCM, washed with water and saturated brine in sequence, dried over Na_2SO_4 and concentrated to give crude sodium **19**, which could be used directly for the next step without further purification.

4.1.22. Benzyl 23-hydroxy-olean[3,2-*d*]-(2-methyl)thiazole-12-en-28-oate (**21a**)

19 (32.0 mg, 50.0 μmol) was dissolved in ethyl alcohol absolute (20.0 mL). Thioacetamide (38.0 mg, 50.0 μmol) was dissolved in ethyl alcohol absolute (20.0 mL) and the solution was dropped into the above solution at a rate of 10 drops per half hour. The reaction was refluxed at 95 °C for 48 h. Ethyl alcohol absolute was removed by vacuum distillation, and the residue was dissolved in DCM, washed with 10% hydrochloric acid solution, saturated sodium bicarbonate solution, water and saturated brine in sequence, dried

over Na₂SO₄ and concentrated. The residue was purified by silica gel column chromatography (V petroleum ether: V ethyl acetate = 10:1) to give a white solid **21a** (24.0 mg, 62.8% yield). m.p. 109.2–113.1 °C. ¹H NMR (400 MHz, CDCl₃) δ 7.34 (s, 5H, 5 × H–Ar), 5.34 (t, J = 3.5 Hz, 1H, H-12), 5.14–5.03 (m, 2H, CH₂Ar), 3.74 (d, J = 10.3 Hz, 1H, H-23a), 3.35 (d, J = 10.3 Hz, 1H, H-23b), 2.93 (d, J = 16.2 Hz, 1H, H-1a), 2.70 (d, J = 15.8 Hz, 1H, H-18), 2.63 (s, 3H, CH₃), 2.24 (d, J = 16.3 Hz, 1H, H-1b), 1.25 (s, 3H, CH₃), 1.14 (s, 3H, CH₃), 0.97 (s, 3H, CH₃), 0.93 (s, 3H, CH₃), 0.90 (s, 3H, CH₃), 0.68 (s, 3H, CH₃); ¹³C NMR (100 MHz, CDCl₃) δ 177.42, 143.81, 136.41, 128.43, 128.04, 127.95, 127.58, 122.13, 71.05, 65.98, 46.90, 46.79, 46.17, 45.87, 41.92, 41.52, 41.46, 39.37, 38.48, 38.35, 33.89, 33.10, 32.34, 31.91, 30.72, 29.70, 28.21, 27.79, 27.63, 25.72, 24.94, 23.62, 23.35, 23.08, 19.79, 19.15, 17.68, 16.65, 15.92; HR-MS (ESI) *m/z*: calcd. for C₃₉H₅₃NO₃S [M+H]⁺: 616.3819, found: 616.3816.

4.1.23. General procedure for the synthesis of **22**

According to the synthesis method of **4**, **15** was deprotected to give crude sodium **20**, which could be used directly for the next step without further purification.

According to the synthesis method of **19**, **20** was reacted with pyridinium bromide perbromide to give crude sodium **22**, which could be used directly for the next step without further purification.

4.1.24. 23-hydroxy-olean[3,2-d]-(2-methyl)thiazole-12-en-28-oic acid (**21b**)

According to the synthesis method of **21a**, **22** was reacted with thioacetamide to give a white solid **21b** (167.0 mg, 64.6% yield) after purified by silica gel column chromatography (V petroleum ether: V ethyl acetate = 1:1). m.p. 121.4–125.2 °C. ¹H NMR (400 MHz, CD₃OD) δ 5.31 (t, J = 3.5 Hz, 1H, H-12), 3.73 (d, J = 10.9 Hz, 1H, H-23a), 3.52 (d, J = 10.9 Hz, 1H, H-23b), 2.91–2.85 (m, 1H, H-1a), 2.73 (d, J = 15.6 Hz, 1H, H-18), 2.63 (s, 3H, CH₃), 2.31 (d, J = 16.0 Hz, 1H, H-1b), 1.21 (s, 3H, CH₃), 1.09 (s, 3H, CH₃), 0.98 (s, 3H, CH₃), 0.95 (s, 3H, CH₃), 0.91 (s, 3H, CH₃), 0.90 (s, 3H, CH₃); ¹³C NMR (100 MHz, DMSO-*D*₆) δ 179.10, 161.32, 154.16, 144.29, 127.78, 122.04, 46.23, 46.05, 46.01, 44.30, 42.48, 42.06, 41.46, 38.34, 33.88, 33.36, 32.60, 31.97, 31.68, 30.94, 30.36, 29.23, 27.78, 25.99, 23.88, 23.35, 23.18, 19.48, 19.30, 18.78, 17.15, 16.04; HR-MS (ESI) *m/z*: calcd. for C₃₂H₄₇NO₃S [M+H]⁺: 526.3350, found: 526.3350.

4.1.25. General procedure for the synthesis of **23**

To a solution of **13** (300.0 mg, 0.4 mmol) in anhydrous DCM (20.0 mL) was added potassium *t*-butoxide (151.0 mg, 1.3 mmol), the reaction was reacted with stirring at room temperature for 2–3 h. Ethyl formate was added when the solution turned brown and the reaction continued overnight. DCM was removed by vacuum distillation, and the residue was dissolved in ethyl acetate, washed with saturated brine, dried over Na₂SO₄ and concentrated to give crude sodium **16**, which could be used directly for the next step without further purification.

To a solution of **16** (334.0 mg, 0.5 mmol) in ethyl alcohol absolute (20.0 mL) was added hydrazine hydrate (0.2 mL, 3.9 mmol), the reaction was refluxed at 80 °C for 4 h. Then water (10.0 mL) was added and ethanol was removed by vacuum distillation, and the residue was dissolved in ethyl acetate, washed with water and saturated brine in sequence, dried over Na₂SO₄ and concentrated. The residue was purified by silica gel column chromatography (V petroleum ether: V ethyl acetate = 5:1) to give a white solid **23** (329.0 mg, 69.9% yield).

4.1.26. Benzyl 23-hydroxy-olean[3,2-*c*]pyrazole-12-en-28-oate (**24a**)

According to the synthesis method of **18**, **23** was deprotected to give a white solid **24a** (225.7 mg, 82.0% yield) after purified by silica

gel column chromatography (V petroleum ether: V ethyl acetate = 2:1). m.p. 132.7–135.7 °C. ¹H NMR (400 MHz, CDCl₃) δ 7.38 (d, J = 4.0 Hz, 5H, 5 × H–Ar), 7.25 (s, 1H, H-pyrazole), 5.39 (t, J = 3.3 Hz, 1H, H-12), 5.12 (q, J = 12.5 Hz, 2H, CH₂Ar), 3.73 (d, J = 10.5 Hz, 1H, H-23a), 3.40 (d, J = 10.5 Hz, 1H, H-23b), 2.97 (d, J = 13.9 Hz, 1H, H-18), 2.60 (d, J = 14.9 Hz, 1H, H-13), 1.24 (s, 3H, CH₃), 1.18 (s, 3H, CH₃), 0.96 (s, 3H, CH₃), 0.94 (s, 3H, CH₃), 0.90 (s, 3H, CH₃), 0.71 (s, 3H, CH₃); ¹³C NMR (100 MHz, CDCl₃) δ 177.49, 149.56, 143.59, 136.39, 131.13, 128.42, 128.01, 127.93, 122.46, 114.08, 70.33, 66.96, 47.48, 46.80, 46.04, 45.96, 41.89, 41.49, 39.28, 38.97, 38.23, 35.84, 33.87, 33.11, 32.34, 31.94, 30.71, 29.70, 29.32, 27.66, 25.71, 23.62, 23.38, 23.08, 19.79, 19.05, 16.66, 15.46; HR-MS (ESI) *m/z*: calcd. for C₃₈H₅₂N₂O₃ [M+H]⁺: 585.4051, found: 585.4040.

4.1.27. 23-hydroxy-olean[3,2-*c*]pyrazole-12-en-28-oic acid (**24b**)

According to the synthesis method of **4**, **24a** was deprotected to give a white solid **24b** (180.5 mg, 87.0% yield) after purified by silica gel column chromatography (V chloroform: V methanol = 6:1). m.p. 122.8–124.1 °C. ¹H NMR (400 MHz, CD₄O) δ 7.91 (s, 1H, NH), 7.21 (s, 1H, H-pyrazole), 5.32 (t, J = 3.3 Hz, 1H, H-12), 3.57 (dd, J = 53.5, 10.9 Hz, 2H, H-23a), 2.90 (d, J = 13.7 Hz, 1H, H-18), 2.59 (d, J = 14.7 Hz, 1H, H-13), 1.21 (s, 3H, CH₃), 1.12 (s, 3H, CH₃), 0.96 (s, 3H, CH₃), 0.92 (s, 3H, CH₃), 0.90 (s, 6H, 2 × CH₃); ¹³C NMR (100 MHz, CD₄O) δ 180.37, 147.13, 143.63, 132.20, 122.26, 114.26, 68.63, 53.34, 46.22, 46.00, 45.87, 41.65, 41.37, 39.09, 38.72, 38.00, 35.55, 33.47, 32.34, 32.14, 31.69, 30.17, 27.45, 24.81, 23.07, 22.65, 22.52, 18.93, 18.18, 16.07, 14.52; HR-MS (ESI) *m/z*: calcd. for C₃₁H₄₆N₂O₃ [M+H]⁺: 495.3581, found: 495.3579.

4.2. Aqueous solubility determination

An excess of each compound was added to 4 mL of deionized water. The suspensions were placed and shaken in a constant temperature oscillator for 24 h at 37 °C, and then the mixtures were centrifuged at 14,000 rpm for 5 min. The supernatants were filtered with 0.45 μm microporous membrane and diluted properly, then the concentration of compounds was determined by UV–Vis spectrophotometry.

4.3. Stability studies

For stability studies, compound **10c** (9 mg, 0.010 mmol) was dissolved in 0.01 M PBS (6 mL, pH 7.4, containing 0.5% Tween 80) and PLE (20 units) was added. The PBS solution was placed and shaken in a constant temperature oscillator at 37 °C. At scheduled time intervals, 1 mL solutions were removed respectively, diluted for 10 times and centrifuged at 14,000 rpm for 5 min. The supernatants were analyzed for compound **10c** by HPLC (LC-20A, Shimadzu, JPN) with UV–Vis detector (SPD-20A) using a ZORBAX SB-C18 column (4.6 × 150 mm, 5 μm) at 37 °C. An isocratic elution method of 95% methanol/water (containing 0.1% trifluoroacetic acid) was applied at a flow rate of 1 mL/min. The concentration of compound **10c** was detected by UV at 306 nm. A reference absorption graph was made from dilution series of the compounds in methanol. The percentage of compound **10c** remaining at each time point relative to the 0 h sample was then calculated from HPLC concentration. Benorylate (9 mg, 0.029 mmol) was dissolved in 0.01 M PBS (17 mL, pH 7.4, containing 0.5% Tween 80) and PLE (57 units) was added. The methods of sample processing and data determination were the same as above, excepted that the isocratic elution method of 56% methanol/water was applied at a flow rate of 1 mL/min.

4.4. Biology

4.4.1. Cell culture

The MDR cancer cell lines KBV and MCF-7T were kindly provided by Dr. Xiaoguang Chen from Institute of Materia Medica, Chinese Academy of Medical Sciences. Both cells were cultured in DMEM medium (Dulbecco's Modified Eagle Medium) with 10% heat-inactivated fetal calf serum, 100 U/mL penicillin and 0.1 mg/mL streptomycin. All cells were incubated at 37 °C in a humidified atmosphere containing 5% CO₂. Moreover, 10 nM paclitaxel was termly added to KBV and MCF-7T medium to keep the drug resistance phenotype. Cells were harvested in the exponential growth phase for further assays.

4.4.2. Cytotoxicity and MDR reversal assay

The viability of cells was tested by the MTT assays as reported previously [47]. In short, cells were seeded in 96-well plates and treated with the tested articles at the desired concentration for 72 h, then cells were treated with MTT solution for about 2 h. After the medium of 96-well plates was discarded, DMSO was added, then the absorbance was measured at 570 nm to calculate the survival rate. The RF which was the index for MDR-reversal activity defined as the ratio between the IC₅₀ value presented by the drugs alone and drugs combined with the test compounds.

4.4.3. Cell cycle distribution analysis

A flow cytometry assay was conducted to analyze the cell cycle distribution as previously reported [48]. Briefly, cells were seeded in 6-well plates, then added the tested compounds to the culture medium for the next day. Cells were harvested after the indicated time, fixed in 80% ethanol overnight at -20 °C, and then washed with PBS and stained with PI solution (20 mg/mL PI and 20 mg/mL RNase in PBS) for 30 min. The cell fluorescence was measured by a flow cytometry machine (BD, C6, USA).

4.4.4. Intracellular rhodamine 123 accumulation assay

The effects of **HBQ** and compound **10c** on the Rhodamine123 accumulation were measured by flow cytometry following our previous protocol [28]. In short, KBV and MCF-7T cells were both treated with or without **HBQ** and compound **10c** for 2 h at indicated concentrations, then both cells were treated with 10 μM Rhodamine123 for 30 min. Subsequently, the cells were harvested and washed with PBS for three times, then detected by flow cytometry machine (BD, C6, USA). 10,000 cells were detected to calculate the mean fluorescence intensity.

4.4.5. Flutax1 fluorescence staining assay

Flutax1 is a fluorescent paclitaxel derivative that binds to the paclitaxel microtubule binding site with high affinity. The KBV and MCF-7T cells were treated with or without compound **10c** for 3 h, then incubated with 1 μM Flutax1 for 1 h. The cells were harvested and washed with PBS for three times, then detected by flow cytometry machine (BD, C6, USA). 10,000 cells were detected to calculate the mean fluorescence intensity.

4.4.6. Molecular docking

The binding mode of compounds and a homology model of human P-gp was constructed and studied via surflex-dock module in software SYBYL-X2.1.1 (Tripos Associates Inc., St. Louis, USA). The three-dimensional structure model of human P-gp protein was derived from the literature [45,46], the binding site of QZ-SSS derived from the crystal structure of mouse P-gp (PDB ID:4M1M) was recognized as the active site of the homology model of human P-gp [45]. The Powell energy gradient method was used for the 3D structure optimization process of all compounds, the force field was

the Tripos force field, and the Gasteiger-Hückel charge was loaded. After protein preparation and molecular optimization, other parameters used system default values to complete the molecular docking process. The docking results were visualized using the PyMOL software (<http://www.pymol.org>).

4.5. Statistical analysis

Date were presented as mean ± SD. The statistical significance of differences between groups was evaluated by the Student's t-test and indicated with **p* < 0.05, ***p* < 0.01.

Declaration of competing interest

The authors declare that they have no known competing financial interests or personal relationships that could have appeared to influence the work reported in this paper.

Acknowledgment

This work was partially supported by National Natural Science Foundation of China (81773563), The Science and Technology Support Program for Youth Innovation in Universities of Shandong (2020KJM003), Natural Science Foundation of Shandong Province (ZR2018LH025), Graduate Innovation Foundation of Yantai University, GIFYTU (YDZD2033), Top Talents Program for One Case One Discussion of Shandong Province. We thank Victoria Muir, PhD, from Liwen Bianji, Edanz Group China (www.liwenbianji.cn/ac), for editing the English text of a draft of this manuscript.

Appendix A. Supplementary data

Supplementary data to this article can be found online at <https://doi.org/10.1016/j.ejmech.2020.113107>.

References

- [1] I.S. Mohammad, W. He, L.F. Yin, Understanding of human ATP binding cassette superfamily and novel multidrug resistance modulators to overcome MDR, *Biomed. Pharmacother.* 100 (2018) 335–348.
- [2] Q. Wu, Z.P. Yang, Y.Z. Nie, Y.Q. Shi, D.M. Fan, Multi-drug resistance in cancer chemotherapeutics: mechanisms and lab approaches, *Canc. Lett.* 347 (2014) 159–166.
- [3] Y.G. Assaraf, A. Brozovic, A.C. Gonçalves, D. Jurkovicova, A. Liné, M. Machuqueiro, S. Saponara, A.B. Sarmiento-Ribeiro, C.P.R. Xavier, M.H. Vasconcelos, The multi-factorial nature of clinical multidrug resistance in cancer, *Drug Resist. Updates* 46 (2019) 100645.
- [4] S. Dallavalle, V. Dobričić, L. Lazzarato, E. Gazzano, M. Machuqueiro, I. Pajeva, I. Tsakovska, N. Zidar, R. Fruttero, Improvement of conventional anti-cancer drugs as new tools against multidrug resistant tumors, *Drug Resist. Updates* 50 (2020) 100682.
- [5] H. Zhang, H.W. Xu, C.R. Ashby, Y.G. Assaraf, Z.S. Chen, H.M. Liu, Chemical molecular-based approach to overcome multidrug resistance in cancer by targeting P-glycoprotein (P-gp), *Med. Res. Rev.* (2020) 1–31.
- [6] E.E. Chufan, H.M. Sim, S.V. Ambudkar, Molecular basis of the polyspecificity of P-glycoprotein (ABC1): recent biochemical and structural studies, *Adv. Canc. Res.* 125 (2015) 71–96.
- [7] R. Silva, V. Vilas-Boas, H. Carmo, R.J. Dinis-Oliveira, F. Carvalho, M.L. Bastos, F. Remiao, Modulation of P-glycoprotein efflux pump: induction and activation as a therapeutic strategy, *Pharmacol. Ther.* 149 (2015) 1–123.
- [8] G. Szakacs, J.K. Paterson, J.A. Ludwig, C. Booth-Genthe, M.M. Gottesman, Targeting multidrug resistance in cancer, *Nat. Rev. Drug Discov.* 5 (2006) 219–234.
- [9] N. Kopcho, G. Chang, E.A. Komives, Dynamics of ABC transporter P-glycoprotein in three conformational states, *Sci. Rep.* 9 (2019) 15092.
- [10] A.K. Nanayakkara, C.A. Follit, G. Chen, N.S. Williams, P.D. Vogel, J.G. Wise, Targeted inhibitors of P-glycoprotein increase chemotherapeutic-induced mortality of multidrug resistant tumor cells, *Sci. Rep.* 8 (2018) 967.
- [11] R.J. Kathawala, P. Gupta, C.R. Ashby, Z.S. Chen, The modulation of ABC transporter-mediated multidrug resistance in cancer: a review of the past decade, *Drug Resist. Updates* 18 (2015) 1–17.
- [12] H.H. Yin, J.J. Dong, Y.C. Cai, X.M. Shi, H. Wang, G.X. Liu, Y. Tang, J.W. Liu, Lei Ma, Design, synthesis and biological evaluation of chalcones as reversers of P-

- glycoprotein-mediated multidrug resistance, *Eur. J. Med. Chem.* 180 (2019) 350–366.
- [13] J. Yu, P. Zhou, J. Asenso, X.D. Yang, C. Wang, W. Wei, Advances in plant-based inhibitors of P-glycoprotein, *J. Enzym. Inhib. Med. Chem.* 31 (2016) 867–881.
- [14] A. Paterna, A. Kincses, G. Spengler, S. Mulhovo, J. Molnár, M. Ferreira, Dregamine and tabernaemontanine derivatives as ABCB1 modulators on resistant cancer cells, *Eur. J. Med. Chem.* 128 (2017) 247–257.
- [15] A. Kumar, V. Jaitak, Natural products as multidrug resistance modulators in cancer, *Eur. J. Med. Chem.* 176 (2019) 268–291.
- [16] B.M.F. Gonçalves, D.S.P. Cardoso, M.J.U. Ferreira, Overcoming multidrug resistance: flavonoid and terpenoid nitrogen-containing derivatives as ABC transporter modulators, *Molecules* 25 (2020) 3364.
- [17] Q.W. Ren, G.Q. Yang, M.Q. Guo, J.W. Guo, Y. Li, J. Lu, Q. Yang, H.H. Tang, Y. Li, X.J. Fang, Y.X. Sun, J.G. Qi, J.W. Tian, H.B. Wang, Design, synthesis, and discovery of ocotillo-type amide derivatives as orally available modulators of P-glycoprotein-mediated multidrug resistance, *Eur. J. Med. Chem.* 161 (2019) 118–130.
- [18] T. Nabekura, T. Yamaki, K. Ueno, S. Kitagawa, Inhibition of P-glycoprotein and multidrug resistance protein 1 by dietary phytochemicals, *Canc. Chemother. Pharmacol.* 62 (2008) 867–873.
- [19] M. Zhou, R.H. Zhang, M. Wang, G.B. Xu, S.G. Liao, Prodrugs of triterpenoids and their derivatives, *Eur. J. Med. Chem.* 131 (2017) 222–236.
- [20] J. Zeng, T. Huang, M. Xue, J.X. Chen, L.L. Feng, R.F. Du, Y. Feng, Current knowledge and development of hederagenin as a promising medicinal agent: a comprehensive review, *RSC Adv.* 8 (2018) 24188–24202.
- [21] C.W. Lee, S.M. Park, R.J. Zhao, C. Lee, W. Chun, Y. Son, S.H. Kim, J.Y. Jung, K.H. Jegal, I.J. Cho, S.K. Ku, Y.W. Kim, S.A. Ju, S.C. Kim, W.G. An, Hederagenin, a major component of *Clematis mandshurica* Ruprecht root, attenuates inflammatory responses in RAW 264.7 cells and in mice, *Int. Immunopharm.* 29 (2015) 528–537.
- [22] D. Zhou, H. Jin, H.B. Lin, X.M. Yang, Y.F. Cheng, F.J. Deng, J.P. Xu, Antidepressant effect of the extracts from fructus akebiae, *Pharmacol., Biochem. Behav.* 94 (2010) 488–495.
- [23] A.G. Wu, W. Zeng, V.K.W. Wong, Y.Z. Zhu, B.Y.K. Law, Hederagenin and α -hederin promote degradation of proteins in neurodegenerative diseases and improve motor deficits in MPTP-mice, *Pharmacol. Res.* 115 (2017) 25–44.
- [24] X.X. Liu, Y.T. Yang, X. Wang, K.Y. Wang, J.Q. Liu, L. Lei, X.M. Luo, R. Zhai, F.H. Fu, H.B. Wang, Y. Bi, Design, synthesis and biological evaluation of novel α -hederagenin derivatives with anticancer activity, *Eur. J. Med. Chem.* 141 (2017) 427–439.
- [25] D. Rodríguez-Hernández, A.J. Demuner, L.C.A. Barbosa, R. Csuk, L. Heller, Hederagenin as a triterpene template for the development of new antitumor compounds, *Eur. J. Med. Chem.* 105 (2015) 57–62.
- [26] K. Fang, X.H. Zhang, Y.T. Han, G.R. Wu, D.S. Cai, N.N. Xue, W.B. Guo, Y.Q. Yang, M. Chen, X.Y. Zhang, H. Wang, T. Ma, P.L. Wang, H.M. Lei, Design, synthesis, and cytotoxic analysis of novel hederagenin–pyrazine derivatives based on partial least squares discriminant analysis, *Int. J. Mol. Sci.* 19 (2018) 2994.
- [27] D. Rodríguez-Hernández, L.C.A. Barbosa, A.J. Demuner, J.P.A. Martins, L. Fischer, R. Csuk, Hederagenin amide derivatives as potential anti-proliferative agents, *Eur. J. Med. Chem.* 168 (2019) 436–446.
- [28] Y.T. Yang, D.K. Guan, L. Leia, J. Lua, J.Q. Liu, G.Q. Yang, C.H. Yan, R. Zhai, J.W. Tian, Y. Bi, F.H. Fua, H.B. Wang, H6, a novel hederagenin derivative, reverses multidrug resistance *in vitro* and *in vivo*, *Toxicol. Appl. Pharmacol.* 341 (2018) 98–105.
- [29] X. Wang, Q.W. Ren, X.X. Liu, Y.T. Yang, B.H. Wang, R. Zhai, J.G. Qi, J.W. Tian, H.B. Wang, Y. Bi, Synthesis and biological evaluation of novel H6 analogues as drug resistance reversal agents, *Eur. J. Med. Chem.* 161 (2019) 364–377.
- [30] W.J. Li, P. Zhan, E.D. Clercq, H.X. Lou, X.Y. Liu, Current drug research on PEGylation with small molecular agents, *Prog. Polym. Sci.* 38 (2013) 421–444.
- [31] J. Hodon, L. Borkova, J. Pokorny, A. Kazakova, M. Urban, Design and synthesis of pentacyclic triterpene conjugates and their use in medicinal research, *Eur. J. Med. Chem.* 182 (2019) 111653.
- [32] A. Kolate, D. Baradia, S. Patil, I. Vhora, G. Kore, A. Misra, PEG—a versatile conjugating ligand for drugs and drug delivery systems, *J. Contr. Release* 192 (2014) 67–81.
- [33] S.A. Senevirathne, K.E. Washington, M.C. Biewer, M.C. Stefan, PEG based anti-cancer drug conjugated prodrug micelles for the delivery of anti-cancer agents, *J. Mater. Chem. B* 4 (2016) 360–370.
- [34] D. Tripathy, S.M. Tolaney, A.D. Seidman, C.K. Anders, N. Ibrahim, H.S. Rugo, C. Twelves, V. Dieras, V. Muller, M. Tagliaferri, A.L. Hannah, J. Cortes, ATTAIN: phase III study of etirinotecan pegol versus treatment of physician's choice in patients with metastatic breast cancer and brain metastases, *Future Oncol.* 15 (2019) 2211–2225.
- [35] M. Medina-O'Donnell, F. Rivas, F.J. Reyes-Zurita, A. Martinez, F. Galisteo-González, J.A. Lupianez, A. Parra, Synthesis and *in vitro* antiproliferative evaluation of PEGylated triterpene acids, *Fitoterapia* 120 (2017) 25–40.
- [36] S.M. Schmitt, K. Stefan, M. Wiese, Pyrrolopyrimidine-derivatives as novel inhibitors of multidrug resistance-associated protein 1 (MRP1, ABCC1), *J. Med. Chem.* 59 (2016) 3018–3033.
- [37] G.A. Patani, E.J. LaVoie, Bioisosterism: A rational approach in drug design, *Chem. Rev.* 96 (1996) 3147–3176.
- [38] N.A. Meanwell, Synopsis of some recent tactical application of bioisosteres in drug design, *J. Med. Chem.* 54 (2011) 2529–2591.
- [39] T. Mosmann, Rapid colorimetric assay for cellular growth and survival: application to proliferation and cytotoxicity assays, *J. Immunol. Methods* 65 (1983) 55–63.
- [40] Y. Ding, Y.Y. Zhou, H. Chen, D.D. Geng, D.Y. Wu, J. Hong, W.B. Shen, T.J. Hang, C. Zhang, The performance of thiol-terminated PEG-paclitaxel-conjugated gold nanoparticles, *Biomaterials* 34 (2013) 10217–10227.
- [41] L. Roux, S. Priet, N. Payrot, C. Weck, M. Fournier, F. Zoulim, J. Balzarini, B. Canard, K. Alvarez, Ester prodrugs of acyclic nucleoside thiophosphonates compared to phosphonates: synthesis, antiviral activity and decomposition study, *Eur. J. Med. Chem.* 63 (2013) 869–881.
- [42] A. Robertson, J.P. Glynn, A.K. Watson, The absorption and metabolism in man of 4-Acetamidophenyl-2-acetoxybenzoate (Benorylate), *Xenobiotica* 2 (1972) 339–347.
- [43] Z. Darzynkiewicz, F. Traganos, L. Staiano-Coico, J. Kapuscinski, M.R. Melamed, Interactions of rhodamine 123 with living cells studied by flow cytometry, *Canc. Res.* 42 (1982) 799–806.
- [44] J.F. Díaz, R. Strobe, Y. Engelborghs, A.A. Souto, J.M. Andreu, Molecular recognition of taxol by microtubules. Kinetics and thermodynamics of binding of fluorescent taxol derivatives to an exposed site, *J. Biol. Chem.* 275 (2000) 26265–26276.
- [45] J. Li, K.F. Jaimes, S.G. Aller, Refined structures of mouse P-glycoprotein, *Protein Sci.* 23 (2013) 34–46.
- [46] S.G. Aller, J. Yu, A. Ward, Y. Weng, S. Chittaboina, R.P. Zhuo, P.M. Harrell, Y.T. Trinh, Q.H. Zhang, I.L. Urbatsch, G. Chang, Structure of P-Glycoprotein reveals a molecular basis for poly-specific drug binding, *Science* 323 (2009) 1718–1722.
- [47] F.F. Li, Z.L. Liu, H.Y. Sun, C.M. Li, W.Y. Wang, L. Ye, C.H. Yan, J.W. Tian, H.B. Wang, PCC0208017, a novel small-molecule inhibitor of MARK3/MARK4, suppresses glioma progression *in vitro* and *in vivo*, *Acta Pharm. Sin. B* 10 (2020) 289–300.
- [48] G.Y. Lv, D.J. Sun, J.W. Zhang, X.X. Xie, X.Q. Wu, W.S. Fang, J.W. Tian, C.H. Yan, H.B. Wang, F.H. Fu, Lx2-32c, a novel semi-synthetic taxane, exerts antitumor activity against prostate cancer cells *in vitro* and *in vivo*, *Acta Pharm. Sin. B* 7 (2017) 52–58.